

SUBMARINE LANDSLIDES AND THEIR TSUNAMI HAZARD

David R Tappin

British Geological Survey, Keyworth, Nottingham, NG12 5GG, United Kingdom

Email: drta@bgs.ac.uk

**Key Words: Tsunami, submarine landslide, hazard, earthquake, volcano, strike-slip
fault**

ABSTRACT

Most tsunamis are generated by earthquakes, fewer from subaerial and submarine landslides, volcanic eruptions, and, rarely, bolide impacts. In 1998, a seabed sediment slump offshore of northern Papua New Guinea generated a tsunami up to 15 m high that killed over 2,200 people. Here we describe how this event changed our understanding of tsunami hazard from submarine landslides, how these are different to earthquakes in tsunami generation, and why they were previously discounted as a major hazard. It was the number of fatalities at PNG that drove the new science, but the understanding of the hazard could not have been achieved without newly developed (multibeam) seabed mapping technology and improved numerical landslide models of tsunami generation. Since 1998, understanding of submarine landslide generation has progressed far beyond anything considered possible at that time. An important aspect of the 1998 event was the contribution made from geologists, to a subject previously dominated by seismologists.

INTRODUCTION

Over the past 20 years' major advances in understanding the mechanisms of tsunami generation have resulted in an improved recognition of their variability, their hazard and their risk. These advances resulted mainly from a number of major, if not devastating, events, together with revisions of older ones. Of critical importance, however, were new technologies available to study the different tsunami mechanisms; including, high-resolution global systems of navigation and seismic networks, high-resolution seabed mapping, improved data recording and storage, and numerical tsunami models. Earthquakes generate the majority (~80%) of tsunamis, and are the best-known mechanism, especially after the Indian Ocean tsunami of 2004, in which 220,000 people died. Although with fewer fatalities than earthquakes, a number

of significant tsunamis resulted from submarine landslides and before 1998 the best known were those of the Grand Banks in 1929 and prehistoric Storegga, at 8,200 years BP (Figure 1).

A new, raised, awareness of the tsunami hazard from submarine landslides resulted after July 1998, when the northern coast of Papua New Guinea (PNG) was devastated by waves of up to 15 m that caused 2,200 fatalities (Kawata et al., 1999). The associated earthquake was not a 'tsunami' earthquake and, with a magnitude M_w 7.1, could not explain the tsunami wave elevations and pattern of inundation (Tappin et al., 1999). During responsive marine surveys, from multibeam echosounder (MBES) bathymetry, seismic and sediment cores offshore the devastated area, a small (6 km^3) sediment failure, a slump, was identified. From the *ad hoc* shipboard, numerical tsunami modelling, this was confirmed as the likely tsunami mechanism (Tappin et al., 1999). The identification of a submarine landslide as the mechanism of a tsunami was controversial (Geist, 2000).

Here we address tsunamis generated from submarine landslides, singly and in association with earthquakes, how these differ from solely earthquake mechanisms, and their impacts. Our focus is on those where there is evidence of tsunamis, rather than all submarine landslides, which are potentially tsunamigenic but without supporting evidence. We show why their hazard was not recognised, before the 1998 PNG event, which led to the recognition of the hazard from submarine landslides. We report on new research on older landslide events along passive and convergent margins, which, benefitting from the realisation at PNG, and new technology and new understandings, improves and refines our understanding of their associated tsunamis and their hazard. We address the tsunamis of Sulawesi and Anak Krakatau in 2018 and finally, why submarine landslide tsunamis, are still less well understood than those from earthquakes, and suggest future approaches to address this deficit.

UNDERSTANDING OF LANDSLIDE TSUNAMIS BEFORE PNG 1998

Tsunamis from submarine landslides are unusual, with limited fatalities compared to those from earthquakes. Before the PNG event, based on theoretical considerations, landslides were considered less efficient than earthquakes in tsunami generation (LeBlond and Jones, 1995). This was surprising because there were a number of well-described landslide tsunamis, such as Grand Banks, Flores Islands and Storegga. The Grand Banks 1929 landslide was known to be triggered by the associated earthquake (Murty, 1977). The Flores Island, 1992, tsunami was mainly generated by an earthquake, which also triggered a landslide (Yeh et al., 1994). Although not proven at the time, there was evidence for a submarine landslide contribution to Aleutian tsunami of 1946 (Johnson and Satake, 1997). Prehistoric landslide tsunamis, included Storegga, dated at 8,150 BP (Harbitz, 1992, Dawson et al., 1988), in the North Atlantic and collapse of the Hawaiian volcanoes in the Pacific, dated at a ~100,000 years BP (Moore and Moore, 1988). Both events were large volume landslides, with no evidence for an associated earthquake contribution, although Storegga was earthquake triggered (Bryn et al., 2005). Other submarine landslide tsunamis included those at Skagway, Alaska, in 1994, where one person died (Kulikov et al., 1996), and at Nice airport, in 1979, where a coastal collapse and triggered a tsunami with one fatality (Assier-Rzadkiewicz et al., 2000).

The evidence for these tsunamis varied. There were eyewitness accounts at Grand Banks and Flores Islands (Clague, 2001, Ruffman and Hann, 2006, Yeh et al., 1993). For Grand Banks, the landslide had been mapped (e.g. Piper et al., 1988) and the landslide mechanism confirmed from earthquake seismograms (Bent, 1995). At Flores Island, there were also field survey coastal observations, measurements of highly elevated tsunami runups of 26 metres at Riangkroko (Yeh et al., 1993), and a numerical model of the tsunami that showed the earthquake could not explain the elevated 26 m runups (Imamura et al., 1995).

With the prehistoric events, the evidence for landslide tsunamis was from sediments deposited as these flooded the land (e.g. Moore and Moore, 1988, Dawson et al., 1988, Felton et al., 2000). For Storegga, the sediments were first identified on the east coast of Scotland, up to 20 metres above present sea level (Dawson et al., 1988). Their identification stimulated a numerical tsunami model, which they validated (Harbitz, 1992). In Hawaii, sediments proposed as deposited by the tsunami from the Alike 2 volcanic collapse, were up to 325 metres above present sea level. A numerical tsunami model found that the proposed landslide mechanism did not generate these tsunami elevations (Johnson and Mader, 1994). An added complication and controversy here, was that the sediments had previously been interpreted as deposited from sea level highstands (Grigg and Jones, 1997).

THE PAPUA NEW GUINEA TSUNAMI – 1998

Initial results and interpretations. The PNG tsunami struck late in the evening of 17th July (Yeh et al., 1994). The tsunami was geographically focussed, flooding 30 km of the coast (Kawata et al., 1999). The M_w 7.1 earthquake was too small to generate the recorded tsunami waves of up to 15 m. It was not a ‘tsunami’ earthquake, using the definition of Newman and Okal based on the discriminant of E/M_0 , (Newman and Okal, 1998), and the aftershock distribution, indicated it was a shallow, not a steeply, dipping thrust, so unlikely to have been the tsunami mechanism (Hurukawa et al., 2003). There was no warning of the tsunami, except the earthquake shaking, hence the 2,200 fatalities. The tsunami was the first devastating event with such a great loss of life for over 20 years, since the Moro Gulf earthquake event in the Philippines in August 1976, where there were over 8,000 fatalities, most (~90%) in the tsunami. The most likely location of the earthquake epicentre was west of the main area of destruction, and close to land <https://www.usgs.gov/centers/pcm/science/descriptive-model-july-17->

1998-papua-new-guinea-tsunami?qt-science_center_objects=0#qt-science_center_objects
https://www.usgs.gov/centers/pcmsc/science/descriptive-model-july-17-1998-papua-new-guinea-tsunami?qt-science_center_objects=0#qt-science_center_objects. From field surveys (Kawata et al., 1999), the geometry of rupture, as inferred from the location of the main shock and aftershocks, was hard to reconcile with the concentration of the devastation to the east of the earthquake epicentre. The 18-minute delay between the earthquake shaking and tsunami impact also indicated that another mechanism was responsible for the event. There were three tsunami waves, with the first causing a withdrawal of the sea, so interpreted as a leading depression wave (Kawata et al., 1999). Succeeding waves were closely spaced, arrived within minutes, and were much smaller than the first. These descriptions were of a highly dispersive wave train, generated by a submarine landslide, rather than the individual waves generated by successive strong components of a sequential seismic rupture. Without marine hydroacoustic data to investigate the event, the tsunami mechanism at that time remained unknown.

Marine surveys and first results on the tsunami mechanism. Because of the large number of fatalities, and the uncertainty over the tsunami mechanism, Japan offered to carry out two marine surveys to acquire seabed bathymetry, seismic and sediment samples north of PNG in the region of the tsunami mechanism. This was the first time after a major tsunami that responsive marine surveys were carried out, so in early 1999, 19,000 km² of 12 kHz multibeam bathymetry (MBES) were acquired offshore northern PNG (Figure 2). In addition, offshore the devastated area, 4.2 kHz sub-bottom seismic (SBS) was also acquired and four, 7 m sediment piston cores (Tappin et al., 1999). From these data, the area offshore northern PNG was interpreted as experiencing significant subduction erosion, resulting in subsidence and collapse of the inner trench slope, which formed the northern margin of the overriding plate. 25 km offshore of the Sissano Lagoon, the area devastated by the tsunami, an amphitheatre-shaped seabed feature, of about 10 km² was identified (Figure 3). This feature was interpreted as

formed by sediment slumping, with a volume of 6 km³. Sediment cores here sampled fine-grained cohesive clays, confirming the likely slump failure mechanism. From still and video seabed photography, acquired by Remotely Operated Vehicle (ROV), fresh fissures and fluid expulsion (Figure 3) from the slump indicated it to be very recent.

The first two marine surveys provided the first indications that the slump in the amphitheatre was the most likely tsunami mechanism (Tappin et al., 1999). Preliminary, *ad hoc*, numerical tsunami models devised onboard the survey vessels, confirmed that an earthquake could not generate the local tsunami, as the faults mapped had normal movement or were too short. The tsunami modelled from the slump generated runups of 5 m, much less, than the maximum 15 m recorded, but this was still considered the more likely tsunami mechanism. Later in 1999, multichannel seismic (MCS) data acquired during a USA funded survey, confirmed the presence of a slump up to 760 m thick within the amphitheatre (Sweet and Silver, 2003). In early 2000, and 2001, two further Japanese funded marine surveys, deployed a manned submersible, Shinkai 3000 and acquired single channel seismic data. The submersible dives within the amphitheatre confirmed recent movement of the slump from sharply defined fissures, concentrations of cold water chemosynthetic communities and fluid expulsion (Figure 3) from the seabed (Tappin et al., 2001) and the seismic data conformed the extent of the slump (Figure 4).

PAPUA NEW GUINEA - CONTROVERSY AND WAKEUP CALL

Immediately after the first two marine surveys, when the initial results on the slump tsunami origin were published, there was some doubt expressed over this conclusion (Geist, 2000). This was mainly because, although there were recognised landslide tsunamis, they were as devastating as PNG. Tsunamis numerically modelled from landslides were rare (Harbitz,

1992). There were a number of aspects to this view; i) the differences in how earthquakes and landslides generate tsunamis – with landslides believed to be too slow and too small, ii) the numerical tsunami models available in 1998 were not suitable for non-seismic mechanisms, and iii) the number of different submarine landslide failure mechanisms (see Geist, 2000). Subsequent numerical modelling, based on additional marine geological and geophysical data and improved numerical models (Tappin et al., 2008, Tappin et al., 2001), validated the tsunami slump mechanism. They were based on improved and validated programmes with the initial condition (wavemaker) from “Tsunami open and progressive initial conditions system” (TOPICS) software, which provided the vertical landslide displacements as outputs, as well as a characteristic tsunami wavelength and a characteristic tsunami period. The dispersive physics of landslide tsunamis was addressed using the Boussinesq propagation models, GEOWAVE (Watts et al., 2003) and the later development, FUNWAVE. These numerical models initially provided tsunami wave elevations offshore, not onland runups, but later modelling provided tsunami wave elevations at the coast (Figure 5). This was a significant improvement over earlier simulations using tsunami source and (non-dispersive) shallow water, tsunami propagation simulations.

How earthquakes and submarine landslides generate tsunamis. Tsunamis are gravity-driven water waves, generated at the water/air interface from a vertical perturbation of the water column. Their velocities are determined by $c = \sqrt{gh}$, where c is celerity, g is gravity ($=9.8 \text{ m/s}^2$) and h water depth. So the deeper the water the faster the tsunami travels. For earthquakes, there are three phases of a tsunami: i) initial wave generation from seabed movement, ii) surface wave collapse, and propagation (travel) across the ocean and, iii) finally, onland incursion or runup (wave elevation at the coast) when the tsunami strikes and flows across land. Earthquake, tsunami-generation models assume initial water surface deformation to be instantaneous and equal to that at the seabed as water is virtually incompressible. For the rise time of most

earthquakes (3-4 km/sec), the long-wave phase velocity in the ocean is slow enough so that displacement is considered instantaneous, as water is almost incompressible. There are slight modifications to the tsunami wave field for earthquakes of slow rupture duration (tsunami earthquakes). Seabed deformation is calculated from earthquake fault parameters using theoretical deformation models, such as Okada (1985).

Submarine landslides generate tsunamis in a similar manner to earthquakes, by a vertical displacement of the seabed that creates a similar displacement at the sea surface (Figure 6). There are, however, several major differences. Landslide displacement much slower with velocities of 10s to 100s of metres a second, the longer source times makes numerical modelling of landslides challenging. The areas of seabed disturbance from submarine landslides are much smaller than those of earthquake rupture; reducing their tsunamigenic potential. Landslide tsunamis are strongly oriented along their direction of movement. There are many different landslide mechanisms, with different morphologies mainly depending on sediment type (Hampton et al., 1996). In the context of tsunami generation, the kinematics of landslide failure can be considered as either blocks or slumps, which on failing, in large part maintain their integrity, or translational, where the sediment disintegrates. The recognition that tsunami generation by landslides is dependent on their failure mechanism, modifies the three elements of tsunami generation used for earthquakes, because there is precursor to tsunami generation, which is the identification of the landslide failure mechanism.

Before PNG, theoretical numerical modelling of tsunamis from submarine landslides was based on a Bingham-type fluid flow, analogous to a translational mechanism, where large blocks, on travelling downslope, disintegrated to form turbidity's (Hampton, 1972, Geist, 2000). Modelling of solid block landslides at the time of the PNG tsunami was in its infancy (Watts, 1998). Numerical tsunami generation models were initially based on depth-averaged wave equations that represented immiscible liquids, or water as a Bingham plastic (Jiang and

LeBlond, 1992, Jiang and LeBlond, 1994). Depth-averaging accurately applies to tsunami generation from earthquakes, but it is questionable when applied to landslide tsunamis, because it does not allow for vertical fluid accelerations, which are important during submarine landslide motion and tsunami generation (Grilli et al., 2002). In 1998, landslide constitutive equations used in numerical models were largely untested by laboratory experiments or by case studies (Tappin et al., 2008). Submarine landslide models were idealised, and not based on geological data (which was generally not available). There was no established method of merging geological data with numerical landslide models. There was little appreciation of the complexity of modelling tsunamis generated from the different submarine landslide mechanisms. For all these reasons, submarine landslides were considered to be ineffective at generating significant tsunamis (Geist, 2000, LeBlond and Jones, 1995). When the PNG tsunami happened, therefore, and the earthquake was an unlikely mechanism, the major challenge was in understanding how the, relatively, slow moving slump submarine landslide generated the tsunami.

POST PNG TSUNAMI DEVELOPMENTS

Despite initial reservations over the landslide mechanism of the PNG tsunami (Geist, 2000), as the results were published, there was an increased interest in the landslide tsunami hazard, especially for events such as Storegga, Grand Banks, and Hawaii, where there was already existing research and interest in their potential hazard.

The prehistoric Storegga landslide tsunami. The Storegga slide (Figure 7) is one of the largest in the world, with a volume of 2,400–3,200 km³ (Haflidason et al., 2004) a slide area of 95,000 km² and a runout distance of 300 km. It failed retrogressively on a very shallow slope of 1-2°. There are a number of landslides at the location of Storegga, each taking place

at the end of each 120,000-year interglacial cycle associated with the waxing and waning of the ice sheets and their associated changes in sea level. This cyclicity also controls landslide triggering (Bryn et al., 2005). The slide had been identified much earlier (Bugge et al., 1987) than PNG, with the associated tsunami identified from sediments deposited on the east coast of Scotland (Dawson et al., 1988). Discovery of these sediments, motivated the first attempt at numerical modelling a submarine landslide tsunami (Harbitz, 1992). The failure model was based on a slide architecture derived from hydroacoustic, and the tsunami runup validated from the east Scotland tsunami sediments. When the PNG tsunami struck, a major investigation into the Storegga tsunami was just beginning because of the discovery, in 1997, of the Ormen Lange gas field beneath the landslide headwall. There was concern that landslide tsunamis could be triggered naturally, or by human induced activities, such as the proposed gas extraction (Solheim et al., 2005). The PNG tsunami, confirmed that this was undoubtedly possible.

Numerical models of the Storegga tsunami post-dating PNG (Bondevik et al., 2005, Hill et al., 2014) were significant improvements on the 1992 research (Harbitz, 1992) as they were based on a more comprehensive data set of geophysics and coring of the landslide (Bryn et al., 2005). In addition, validation of later numerical models was from a more extensive tsunami sediment runup data from Norway (Bondevik et al., 1997), Faroe Islands (Grauert et al., 2001), Shetland Islands (Bondevik et al., 2003) and mainland Scotland (Smith et al., 2007). The later numerical models, reproduced the maximum tsunami runups on the Shetlands sediments, which were up to 20 m above present sea level, and probably higher (~30 m) above the sea level at the time of the slide (Bondevik et al., 2005). Even with the large scale resources expended on Storegga, however, there were still uncertainties over the relationships between the landslide and tsunami generation (Solheim et al., 2005).

Most recently, further numerical modelling of large volume landslides on the Norwegian margin including Storegga and Trænadjupet, located farther north, has resulted in advances in model development. There has been a raised interest in the tsunami hazard from very large volume landslides and their hazard in the North Atlantic that may be increased by global warming (Løvholt et al., 2017, Hill et al., 2014, Løvholt et al., 2015). These new studies have led to new insights into landslide tsunamis that include; i) large volume landslides do not necessarily generate tsunamis commensurate with their size , ii) tsunamis generated from long runout distances of translational large volume landslides such as Storegga may not be dispersive (Glimsdal et al., 2013), and iii) retrogressive failure is a critical control on tsunami generation. Overall, the research demonstrates the critical importance of landslide morphology in tsunami modelling, both in representing the failure mechanism and the resulting tsunami elevation and extent. It is critically important therefore to use appropriate landslide mechanisms in numerical tsunami modelling. Other important factors controlling tsunami generation include slide velocity, slide volume, failure mechanism, water depth and slide distance from shoreline. Further, blocks and slumps are impulsive events and it is their velocity that is most important in initial tsunami generation, whereas with translational landslides it is their acceleration (Løvholt et al., 2015). Generally, translational landslides are larger volume, with longer runout distances compared to blocks and slumps. These large volume landslides are generally considered retrogressive, failing from the bottom up, a mechanism, which reduces their tsunamigenic potential. The research confirms that even large volume landslides, may produce tsunamis of modest size and that depth averaging may not be as important in large volume landslide numerical tsunami models as previously believed.

The Hawaiian Giant Submarine Landslides (GSLs). The PNG tsunami resulted in further research on the Hawaiian GSLs, to ascertain their tsunami hazard, by focussing on the origin of the elevated tsunami deposits, and numerical tsunami modelling of the collapse of the

120,000 years BP, Alika 2 GSL (Figure 8). Detailed sedimentology and age dating on the sedimentary deposits on Lana'i and Moloka'i, Hawaii (Rubin et al., 2000, Moore, 2000), seemed not to resolve whether they were deposited from highstands (Stearns, 1978) or tsunamis, as proposed by Moore and Moore (Moore and Moore, 1988). Research on similar deposits on the Big Island of Hawaii (McMurtry et al., 2004a), however, demonstrated that these resulted from a tsunami with an elevation of ~400 m above sea level at time of deposition. The 120,000 years BP age of both deposits and the offshore Alika 2 GSL, indicated a strong genetic link, suggesting that this was the tsunami mechanism. Numerical tsunami modelling of the landslide confirmed this as the source of the sediment producing local elevations of 100s of metres. It demonstrated that the large volume volcanic GSLs were a potential major tsunami hazard, with their triggering related to global warming and cooling climate changes over the past 100s of thousands of years (McMurtry et al., 2004b).

The Grand Banks tsunami of 1929. Research on the Grand Banks event up to 1998 had mapped (Heezen and Ewing, 1952, Piper et al., 1988), but a numerical model of the tsunami was not attempted until afterward, and in fact was stimulated by PNG (Fine et al., 2005). 28 people drowned in the tsunami, which was caused by a landslide triggered by the earthquake (Heezen and Ewing, 1952, Fine et al., 2005). Its strike slip mechanism and magnitude, M_w 7.2, however, was too small to generate the tsunami (Bent, 1995). Strike slip earthquakes rarely cause the seabed vertical movement necessary to generate large tsunamis. At shallow water depths, the earthquake broke submarine telephone cables, but sequential, deeper water, breaks resulted from sediment movement. The sediment failure covers 5,200 km² with 200 km³ of sediment deposited over 150,000 km² (Piper et al., 1988). The initial failure was small, but triggered numerous, overlapping, thin failures. As with Storegga, the slide was translational and retrogressive. Although nearly 100 years old, and well studied, the landslide had, until recently, only been mapped with backscatter data, from which seabed sediment type and

morphology can be interpreted, and sediment sampling. It was not until this century that MBES bathymetry was acquired, which was used in new numerical tsunami modelling (Schulten et al., 2018, Løvholt et al., 2018, Mosher and Piper, 2007).

Previous modelling of Grand Banks (Fine et al., 2005) was based on a viscous incompressible fluid, and non-dispersive physical model. From the new MBES and seismic data, the landslide was hard to define (Mosher and Piper, 2007) as there was no evidence of a single large landslide nor a major headscarp or debris lobe. It is a complex association of shallow, seabed failures, triggered by the earthquake (Schulten et al., 2018). The surficial sediment failures are concentrated along deep-water escarpments. They comprise widely distributed, translational, retrogressive, slump failures that liquefied into debris flows, which rapidly evolved into a massive channelized turbidity current. The slump head scarps are 100 m in elevation. Their deep-water location and retrogressive failure make them unlikely as a main tsunami mechanism. This suggests that the shallow water, localized fault scarps generated the tsunami. Numerical modelling of the tsunami, based on the new hydroacoustic data, shows that the shallow slumps generated the elevated tsunami run-ups observed locally, in Newfoundland, and the translational landslides the longer-period waves observed in the far field (Løvholt et al., 2018).

RECENT DEVELOPMENTS – DUAL MECHANISM TSUMAMIS

Over the past 5 to 10 years, there has been a resurgence in interest in landslide tsunamis. In large part, this resulted from new developments in numerical models of submarine landslide tsunamis, which are based on their different failure mechanisms, which generate dispersive tsunamis. These new models have resulted in improvements beyond solid block landslides modelled as earthquakes. A major contributory factor has been the increased availability of

MBES bathymetry that provides much improved, high resolution, imaging of seabed morphology. Older events, such as Grand Banks, Storegga, Messina, 1908 and Puerto Rico, 1918 have been revisited. In March 2011, however, another catastrophic tsunami struck that, despite the warning from the Indian Ocean seven years previously, arrived unexpectedly in another completely different context and devastated the country best prepared for tsunamis in the world - Japan.

Japan Tsunami March 11th 2011. The Japan 2011 tsunami was another challenging event where, although the earthquake was large at M_w 9.1, there is evidence that this may not have generated all the recorded tsunami. The tsunami struck the east coast Honshu. The earthquake magnitude was unpredicted, so the tsunami was far higher and more destructive than expected. Over 18,000 people perished. Because of its magnitude, the earthquake was immediately interpreted as the single tsunami mechanism, but it could not explain the elevated (40 m) and focused tsunami run-ups along the Sanriku coast on northern Honshu Island north of latitude 39°N (e.g. Fujii et al., 2011, MacInnes et al., 2013). In addition, inversion of tsunami waveforms, could not reproduce the timing and high-frequency content of tsunami waveforms recorded at the nearshore GPS buoys located offshore Sanriku, nor the timing of the dispersive-wave train at the Deep-Ocean Assessment and Reporting of Tsunamis (DART) buoy #21418 located 600 km off the coast (e.g. Grilli et al., 2013).

The high frequency content of the tsunami waveforms recorded by bottom sensors offshore the northern region of the rupture, together with the elevated runups north of the main rupture, suggested there could be an additional mechanism. Tappin et al. (Tappin et al., 2014), based on a comprehensive analysis of the event and numerical modelling, suggested this mechanism was a submarine landslide located east of the highest runups (Figure 9). From MBES bathymetry, a landslide was identified, and numerical modelling of the dual tsunami mechanism, earthquake and submarine landslide, reproduced the elevated tsunami waves along

the Honshu coast better than the earthquake on its own, especially in the north of the inundated area, in the Sanriku region. Support for the landslide mechanism came from farther south, where other landslides triggered by the 2011 earthquake, were identified (Figure 9), but too far south of the region of elevated onshore run-ups (Kawamura et al., 2012).

The 2011 dual tsunami mechanism, however, remains controversial, with recently published earthquake numerical tsunami simulations suggesting alternatives to the dual mechanism, but not completely discounting it (Yamazaki et al., 2018, Lay, 2018). In addition, bathymetric data acquired after the submarine landslide mechanism was proposed (Fujiwara et al., 2017), reveals no evidence for the size of submarine landslide displacement at the location proposed. Notwithstanding the absence of a major landslide at this location, there are seabed failures identified in the northern area of the 2011 earthquake rupture, and farther north, on both before and after 2011 MBES bathymetry and multichannel seismic (MCS) (Tappin et al., 2014, Boston et al., 2017). On the prism margin, at the location of the slump proposed by Tappin et al., simulations based on the inversion of tsunami wave data, identify anomalous seabed movement, which is not explained. A major hindrance to identifying seabed movement here, in the region north of 39.5°N, is the lack of post-event MBES bathymetry, which could answer the problem. On the pre-2011 MBES data, there are landslides in this region (Figure 9), so new MBES bathymetry is essential to identify what the movement is.

Dual mechanism – other events. Japan, perhaps, raised the profile of dual mechanism tsunamis where earthquakes and submarine landslides might be involved and, with MBES bathymetry increasingly available, it is possible in many instances to address these events. The tsunami mechanisms of Messina, 1908 and Puerto Rico, 1918 have been subject to controversy for over 100 years (López-Venegas et al., 2008, Schambach et al., 2020). With Puerto Rico, there was historical evidence of landsliding from the breakage of submarine telegraph cables. MBES bathymetry showed evidence of a submarine landslide which, together with numerical

tsunami modelling, now confirms the landslide mechanism of the tsunami (López-Venegas et al., 2008).

At Messina, 1908 sediment movement was evident from submarine cable breakages (Ryan and Heezen, 1965.) together with coastal landslides and here, seabed movement was proposed soon after the event (Omori, 1909). The earthquake and tsunami were catastrophic, with ~60,000 fatalities. The earthquake, restricted to the north of the Ionian Sea in the Messina Strait, could not explain, the tsunamis up to 12 m in elevation recorded much farther south along the east coast of Sicily and on the south coast of Calabria. A landslide was identified offshore of Mount Etna, (Billi et al., 2008), and numerical modelling based on hypothetical mechanisms supported this interpretation (Favalli et al., 2009). More recently, from MBES bathymetry, a slide block, identified offshore of Mount Etna, was the basis is for numerical tsunami simulations, and this suggests that this, in addition to the earthquake, contributed to the tsunami in the southern region (Schambach et al., 2020). Tsunami elevations farther north toward the Messina Strait are from additional landslides, perhaps coastal, on Sicily and Calabria, which were reported at the time (Baratta, 1910). The dual mechanism of the EQ and a block landslide offshore Mount Etna a location consistent with earlier studies, and a fairly rigid-block-slump, rather than a translational SMF. Tsunami generation and its propagation to shore, is based on higher resolution grids and accurate bathymetry and topography than in earlier work. Runups and travel times agree well with observations, except for runups on either side of the Messina Straits north of the SMF, which are still under predicted. As with all previous modelling of this event, additional mechanisms are required to explain runups in the northern Messina Straits, which we suggest might be smaller and shallower SMFs located in this area.

RECENT EVENTS IN INDONESIA 2018

Towards the end of 2018, two destructive tsunamis struck Indonesia, one in Sulawesi in September and a second in the Sunda Strait between Java and Sumatra. The mechanisms of these events were very different, with the first associated with a strike slip earthquake and the second, a volcanic eruption. The Sulawesi tsunamis were up to 10-11 metres in elevation, much larger than expected from the earthquake mechanism, but observations from field studies suggested that coastal landslides were an important mechanism. At Anak Krakatau, it was obviously a flank collapse that generated the tsunami, with most data on the subaerial collapse but as yet, there are few published data on the submarine aspects.

Both recent Indonesian tsunamis flag the hazard from non-seismic tsunami mechanisms, and how few case studies there are. Anak Krakatau is important because it is the first volcanic flank collapse tsunami since Krakatau, in the late 19th century and the first major event where there is an opportunity to utilise modern technology to map the subaerial and submarine parts of the collapse. The last major eruption tsunami was at the same location, the famous event of 1883, when there were 36,000 fatalities.

Sulawesi (Palu) tsunami 28th September 2018. A M_w 7.5 supershear, earthquake struck Central Sulawesi, Indonesia, on September 28, 2018, rapidly followed by a destructive tsunami in Palu Bay (Bao et al., 2019, Socquet et al., 2019). The earthquake was predominantly strike-slip, so at first sight could not explain the maximum 11 m runups recorded in the southern part of the bay, confirmed by most published earthquake models, which predicted limited vertical deformation. Some papers identified several metres of vertical uplift, but not in the Bay, farther north (Song et al., 2019). Others (Ulrich et al., 2019) suggested that the

strike slip mechanisms along steeper sides of the Bay resulted in an apparent greater uplift as proposed by Tamaki and Satake (1996).

Responsive field surveys after the event identified numerous small coastal landslides (Figure 11, which offered an alternative tsunami mechanism (Arikawa et al., 2018, Muhari et al., 2018, Nakata et al., 2020). Therefore, there was debate over whether the tsunami was generated by an earthquake, coastal landslides, or a combination of both. Early publications on the tsunami were inconclusive in this regard, some identifying the earthquake as explaining most tsunami observations, with others disregarding the earthquake contribution entirely and focusing solely on landslide sources, but these were based on hypothetical landslides, not confirmed by post-tsunami bathymetric surveys (Pakoksung et al., 2019).

The most recent research (Schambach et al., in review) models the tsunami from a combination of earthquake ruptures (based on Jamelot et al., 2019, Socquet et al., 2019, Ulrich et al., 2019), which vary in their basis and complexity, coastal landslides mapped from field and video evidence of the tsunami impact, together with marine bathymetric surveys. It uses a combination of two numerical models generating the tsunami and propagating the waves, the 3D non-hydrostatic wave model NHWAVE and the 2D Boussinesq wave model FUNWAVE-TVD. The new models are important because they are these are only ones including the physics of wave frequency dispersion, which is important for modeling landslide generated tsunamis. The coastal landslides were modeled in NHWAVE as granular material. The results from combined earthquake and coastal landslide models recreate the recorded and observed tsunami runups around the Bay, except in the southeast, where there were the most elevated (11m) runups. A major challenge in recreating the tsunamis was the timing of impact from the local coastal landslides. Here, for the first time, there is reasonable agreement between the landslide plus earthquake models of Socquet et al. (2019) and Ulrich et al. (2019) and the timing of impact at several locations around the bay. The results confirm that to explain the tsunami in the southeast

of Palu Bay local mechanisms additional to the earthquake are required, and that these are the observed coastal landslides.

Anak Krakatau, December 22nd 2018. At approximately 20:56 local time on the 22nd, Anak Krakatau volcano, in the Sunda Straits, Indonesia, experienced a major lateral collapse during a period of eruptive activity that began in June (Walter et al., 2019). The collapse, into the 250 m deep caldera graben, located on the southwest flank of the volcano generated a tsunami up to 40 m in elevation within the caldera, with runups of up to 13 m on the adjacent coasts of Sumatra and Java (Grilli et al., 2019) (Figure 12). There were 437 fatalities, the greatest loss of life in a volcanic tsunami since the catastrophic explosive eruption of Krakatau in 1883 and the sector collapse of Ritter Island in 1888. For the first time in over 100 years, the event provided an opportunity to study a major volcanic tsunami with widespread loss of life and significant damage. The eruption of Anak Krakatau is closely linked to that of 1883 because the volcano developed within the remains of the Krakatau caldera largely destroyed in that cataclysmic eruption. From a submarine volcano in the northeast margin of the caldera, it developed into a subaerial edifice, with a pre-2018 collapse height of about 335 m. The growth and collapse of Anak Krakatau was due to three reasons (Grilli et al., 2019):

- i) its location above NNE-SSW trending feeder vents that control volcanic activity of the volcano,
- ii) the location of Anak Krakatau on the northeast margin of the deep 250 m deep graben in the west of the caldera, and
- iii) the gradual migration of Anak Krakatau towards the edge of the graben since the 1883 Krakatau eruption.

The landslide formed mainly of large blocks of subaerially erupted lavas (Figure 13), which were emplaced on friable submarine erupted pyroclastics, which were therefore inherently unstable (Hunt et al., in review). The eruption triggered the collapse. From pre- and post-event

satellite images and aerial photography, 50% of Anak Krakatau volcano, failed into the graben causing a landslide between 0.22–0.30 km³ in volume. This was used to initialize the tsunami generation and propagation model with two different landslide rheologies (granular and fluid) (Grilli et al., 2019). Observations of a single tsunami, with no subsequent waves, are consistent with our interpretation of landslide failure in a rapid, single phase of movement rather than a more piecemeal process, generating a tsunami, which reached nearby coastlines within ~30 minutes. Both modelled rheologies successfully reproduce observed tsunami characteristics from post-event field survey results, tide gauge records, and eyewitness reports, suggesting our estimated landslide volume range is appropriate. The event highlights the significant hazard from relatively small-scale lateral volcanic collapses, which can occur without any precursory signals, and are an efficient and unpredictable tsunami source. The absence of precursory warning signals together with the short travel time following tsunami initiation present a major challenge for mitigating tsunami coastal impact.

SUBMARINE LANDSLIDE TSUNAMI – THE HAZARD REMAINS UNDEFINED

Before PNG, submarine landslides were not considered a major tsunami hazard, if they were considered at all. High impact, low frequency hazards, such as earthquakes and tsunamis are a major challenge, because of the cost of investigation. Major storms for example take place several times a year, but with events that strike every 50 to 100 years, if not over longer time intervals, it takes a major disaster both to excite interest and attract research funding. Where the hazard has not previously been recognised, as in 1998 with submarine landslide tsunamis, it is even more challenging. Even though submarine and subaerial landslide tsunamis had been known for many years, it took a major disaster, with 2,200 fatalities to identify the hazard. This

is not too different to earthquake tsunamis. In the Indian Ocean tsunami in 2004, 220,000 people died, 170,000 in Aceh, close to the epicentre, so no chance of evacuation. But, the other 50,000 in India, Thailand and Sri Lanka, should not have died, but there was no warning system. The last great EQ was Valdivia in 1960, so the science in 2004 was outdated, and the EQ hazard in the region underestimated (Ruff and Kamamori, 1980). Whereas here EQs were a well-established hazard in the Indian Ocean it was the location and the scale.

Over the period since the 1998 PNG event the tsunami hazard from submarine landslides has been increasingly accepted and widely recognized. After the initial controversy over the mechanism, PNG has been transformative in this major advance. The extensive mapping of continental margins shows that submarine landslides are commonly present (Figure 1). Along passive margins, exemplified by Storegga, there is a strong climate control on sediment failure. Research suggests that failure is related to sedimentation regimes controlled in part by the 120 000-year, interglacial/glacial cycles, with triggering mainly from earthquakes. The dominant controls on landslides along convergent margins are not as well established, but probably dominated by local sedimentation regimes, with triggering from earthquakes. Five years ago, only four major submarine landslide tsunamis had been identified, researched and validated: Storegga, Grand Banks, Papua New Guinea and Japan (Tappin, 2017). As can be seen here since this time more events have been identified as generated from submarine landslides or are dual mechanism and older events, such as Grand Banks and Storegga better studied and understood. Other events where there is a suspicion of a landslide influence such as Makran (1945), Aleutians (1946), Alaska (1964), Flores Islands (1992) and Java (2006), still require further research to understand their specific mechanisms, so remain enigmatic.

Along convergent margins one of the most tantalising challenges is the definition on ‘tsunami’ earthquakes. Identified in 1972 (Kanamori, 1972), at these events the tsunamis generated, are much larger than expected from their associated earthquake surface wave magnitudes. Two

events provided the basis for the identification, Sanriku, 1893, and the Aleutians tsunami of 1946. An important proviso, identified in the paper, was that these tsunamis, alternatively, could have been associated with submarine landslides and, as noted above for the 1946 event, evidence published later suggested that indeed, a submarine landslide was probably involved (Johnson and Satake, 1997). There is evidence in the region of the 1893 event for submarine landslides (Tappin et al., 2014) and it has now been demonstrated that the local tsunami of 1946 was also likely generated by a landslide (Fryer et al., 2004)

There is a new reality, which has somewhat dampened the early optimism on just finding and mapping SMFs, then modelling them, to the realisation that even large volume slides may not be as visible as previously been conceived (Mosher and Piper, 2007). Dual mechanism tsunamis are a newly realised challenge, flagged by Japan, 2011, and with the new published research on Messina, 1908 (Schambach et al., 2020). It has been recognised that for some time that the earthquake could not generate the extensively recorded tsunami (Tinti and Armigliato, 2003). New numerical modelling in part answers some of the problems (Schambach et al., 2020), but not all as there is an earthquake in the north a submarine landslide mechanism off Mount Etna, and additional landslides in the north, off Sicily and Calabria. The MBES bathymetry in the north, shows no good evidence for submarine landslide, so it is a scenario similar to the Grand Banks. For Messina however, there were numerous landslides associated to the earthquake and some of these were on the coast of Sicily and Calabria, which leads on to the recent events in Indonesia, on Sulawesi and Krakatau.

At Sulawesi, the evidence for a dual mechanism tsunami was apparent from the outset, because of the strike slip fault mechanism, and the reports of coastal landslides from the field surveys, with the sequence of events, earthquake, coastal landslides and tsunamis taking place in rapid succession (Carvajal et al., 2019). 20 years earlier, acceptance of this possibility would have been unlikely. Now, there is controversy over the tsunami mechanisms but landslides are

undoubtedly part of the discussion. With Anak Krakatau it is similar, volcanic collapse is accepted as a possible tsunami mechanism from research in Hawaii and also on the Canary Islands on the far field hazard to the east coast of the United States (Abadie et al., 2012).

There are now a number of well-studied submarine landslide tsunamis, on passive, convergent strike slip margins and on volcanoes. Over the past 20 years, understanding of landslide mechanisms has advanced significantly. One the lessons learned is that, compared to earthquakes, the variety of landslide-generated tsunamis is endless. Looking at Figure 1, and comparing the number of landslide events in the context of the length of the oceanic margin where landslides are located, there is a long way to go before their hazard is understood the level that mitigation can be considered.

FUTURE DIRECTIONS OF RESEARCH

There are now a number of submarine landslides identified and studied, but still too few well-understood. Based on this review, there are a number of directions are identified to advance our understanding of their mechanisms and their hazard.

There needs to be a closer collaboration between geoscientists and numerical modellers so that simulations are well founded in geological reality.

There needs to be a greater realisation of the limitations of numerical models appropriate to earthquake tsunamis used to simulate landslides.

There needs to be a greater awareness that landslide tsunami simulations should be validated, either by eyewitness observations and field surveys in the case of historical events, or tsunami sediments for older events.

As exemplified by Sulawesi, where there is timing information on tsunami impact, this is critical in discrimination mechanisms where there is the possibility of more than one.

There needs to be more research on well-studied events to validate existing models.

ACKNOWLEDGEMENTS

Many thanks to all my numerous colleagues who I have worked on tsunamis with, both in the field and lab, over the past 20 years. The paper contains satellite imagery from Google Earth, Digital Globe open data for disaster response, and Sentinel-2 cloudless data (<https://s2maps.eu> by EOX IT Services GmbH; containing modified Copernicus Sentinel data 2017 and 2018). The author publishes with the permission of the CEO of the British Geological Survey (United Kingdom Research and Innovation).

REFERENCES

- ABADIE, S. M., HARRIS, J. C., GRILLI, S. T. & FABRE, R. 2012. Numerical modeling of tsunami waves generated by the flank collapse of the Cumbre Vieja Volcano (La Palma, Canary Islands): Tsunami source and near field effects. *J. Geophys. Res.*, 117, C05030.
- ARIKAWA, T., MUHARI, A., OKUMURA, Y., DOHI, Y., AFRIYANTO, B., SUJATMIKO, K. A. & IMAMURA, F. 2018. Coastal Subsidence Induced Several Tsunamis During the 2018 Sulawesi Earthquake. *Journal of Disaster Research*, sc20181204-sc20181204.
- ASSIER-RZADKIEWICZ, S., HEINRICH, P., SABATIER, P. C., SAVOYE, B. & BOURILLET, J.-F. 2000. Numerical modelling of a landslide-generated tsunami: the 1979 Nice event. *Pure and Applied. Geophysics*, 157, 1707-1727.

- BAO, H., AMPUERO, J.-P., MENG, L., FIELDING, E. J., LIANG, C., MILLINER, C. W. D., FENG, T. & HUANG, H. 2019. Early and persistent supershear rupture of the 2018 magnitude 7.5 Palu earthquake. *Nature Geoscience*, 12, 200-205.
- BARATTA, M. 1910. *La Catastrofe Sismica Calabro-Messinese (28 Dicembre 1908)*.
- BENT, A. L. 1995. A complex double-couple source mechanism for the Ms 7.2 1929 Grand Banks earthquake. *Bulletin of the Seismological Society of America*, 85, 1003-1020.
- BILLI, A., FUNICIELLO, R., MINELLI, L., FACCENNA, C., NERI, G., ORECCHIO, B. & PRESTI, D. 2008. On the cause of the 1908 Messina tsunami, southern Italy. *Geophysical Research Letters*, 35.
- BONDEVIK, S., LØVHOLT, F., HARBITZ, C., MANGERUD, J., DAWSON, A. & SVENDSEN, J. I. 2005. The Storegga Slide tsunami—comparing field observations with numerical simulations. *Marine and Petroleum Geology* 22, 195–208.
- BONDEVIK, S., MANGERUD, J., DAWSON, S., DAWSON, A. & LOHNE, Ø. 2003. Record-breaking height for 8000-year-old tsunami in the North Atlantic. *EOS, Transactions American Geophysical Union*, 84, 289-293.
- BONDEVIK, S., SVENDSEN, J. I. & MANGERUD, J. A. N. 1997. Tsunami sedimentary facies deposited by the Storegga tsunami in shallow marine basins and coastal lakes, western Norway. *Sedimentology*, 44, 1115-1131.
- BOSTON, B., MOORE, G. F., NAKAMURA, Y. & KODAIRA, S. 2017. Forearc slope deformation above the Japan Trench megathrust: Implications for subduction erosion. *Earth and Planetary Science Letters*, 462, 26-34.
- BRYN, P., BERG, K., FORSBERG, C. F., SOLHEIM, A. & LIEN, R. 2005. Explaining the Storegga Slide. *Marine and Petroleum Geology*, 22, 11-19.

- BUGGE, T., BEFRING, S., BELDERSON, R. H., EIDVIN, T., JANSEN, E., KENYON, N. H., HOLTEDAL, H. & SEJRUP, H. P. 1987. A giant three stage submarine slide off Norway. *Geomar. Lett*, 7, 191–198.
- CARVAJAL, M., ARAYA-CORNEJO, C., SEPÚLVEDA, I., MELNICK, D. & HAASE, J. S. 2019. Nearly Instantaneous Tsunamis Following the Mw 7.5 2018 Palu Earthquake. *Geophysical Research Letters*, 46, 5117-5126.
- CLAGUE, D. 2001. Tsunamis. In: BROOKS, G. R. (ed.) *A Synthesis of Geological Hazards in Canada*. Canada: Geological Survey of Canada Bulletin.
- DAWSON, A. G., LONG, D. & SMITH, D. E. 1988. The Storegga Slides: evidence from eastern Scotland for a possible tsunami. *Marine Geology*, 82, 271–276.
- MARINE INFORMATION SERVICE. 2016. EMODnet Digital Bathymetry (DTM). Marine Information Service <https://doi.org/10.12770/c7b53704-999d-4721-b1a3-04ec60c87238>.
- FAVALLI, M., BOSCHI, E., MAZZARINI, F. & PARESCHI, M. T. 2009. Seismic and landslide source of the 1908 Straits of Messina tsunami (Sicily, Italy). *Geophys. Res. Lett.*, 36, L16304.
- FELTON, E. A., CROOK, K. A. W. & KEATING, B. H. 2000. The Hulopoe gravel, Lanai, Hawaii: New sedimentological data and their bearing on the ‘giant wave’ (mega-tsunami) emplacement hypothesis. *Pure Appl. Geophys*, 157, 1257-1284.
- FINE, I. V., RABINOVICH, A. B., BORNHOLD, B. D., THOMSON, R. E. & KULIKOV, E. A. 2005. The Grand Banks landslide-generated tsunami of November 18, 1929: preliminary analysis and numerical modeling. *Marine Geology*, 215, 45-57.
- FRYER, G. J., WATTS, P. & PRATSON, L. F. 2004. Source of the great tsunami of 1 April 1946: a landslide in the upper Aleutian forearc. *Marine Geology* 203, 201-218.

- FUJII, Y., SATAKE, K., SAKAI, S. I., SHINOHARA, M. & KANAZAWA, T. 2011. Tsunami source of the 2011 off the Pacific coast of Tohoku Earthquake. *Earth Planets Space*, 63, 815–820.
- FUJIWARA, T., DOS SANTOS FERREIRA, C., BACHMANN, A. K., STRASSER, M., WEFER, G., SUN, T., KANAMATSU, T. & KODAIRA, S. 2017. Seafloor Displacement After the 2011 Tohoku-oki Earthquake in the Northern Japan Trench Examined by Repeated Bathymetric Surveys. *Geophysical Research Letters*, 44, 11,833-11,839.
- GEIST, E. L. 2000. Origin of the 17 July, 1998 Papua New Guinea tsunami: Earthquake or landslide? *Seis. Res. Lett.*, 71, 344–351.
- GLIMSDAL, S., PEDERSEN, G. K., HARBITZ, C. B. & LØVHOLT, F. 2013. Dispersion of tsunamis: does it really matter? *Nat. Hazards Earth Syst. Sci.*, 13, 1507-1526.
- GRAUERT, M., BJÖRCK, S. & BONDEVIK, S. 2001. Storegga tsunami deposits in a coastal lake on Suouroy, the Faroe Islands. *Boreas*, 30, 263-271.
- GRIGG, R. W. & JONES, A. T. 1997. Uplift caused by lithospheric flexure in the Hawaiian Archipelago as revealed by elevated coral deposits. *Marine Geology*, 141, 11-25.
- GRILLI, S. T., HARRIS, J. C., BAKHSH, T. S. T., MASTERLARK, T. L., KYRIAKOPOULOS, C., KIRBY, J. T. & SHI, F. 2013. Numerical Simulation of the 2011 Tohoku Tsunami Based on a New Transient FEM Co-seismic Source: Comparison to Far- and Near-Field Observations. *Pure and Applied Geophysics*.
- GRILLI, S. T., TAPPIN, D. R., CAREY, S., WATT, S. F. L., WARD, S. N., GRILLI, A. R., ENGWELL, S. L., ZHANG, C., KIRBY, J. T., SCHAMBACH, L. & MUIN, M. 2019. Modelling of the tsunami from the December 22, 2018 lateral collapse of Anak Krakatau volcano in the Sunda Straits, Indonesia. *Scientific Reports*, 9, 11946.

- GRILLI, S. T., VOGELMANN, S. & WATTS, P. 2002. Development of a 3D numerical wave tank for modelling tsunami generation by underwater landslides. *Engrg. Analysis with Boundary Elements*, 26(4), 301–313.
- HAFLIDASON, H., SEJRUP, H. P., NYGÅRD, A., MIENERT, J., BRYN, P., LIEN, R., FORSBERG, C. F., BERG, K. & MASSON, D. 2004. The Storegga Slide: architecture, geometry and slide development. *Marine Geology*, 213, 201-234.
- HAMPTON, M. 1972. The role of subaqueous debris flow in generating turbidity currents. *J. of Sed. Petr.*, 42, 775–993.
- HAMPTON, M. A., LEE, H. J. & LOCAT, J. 1996. Submarine Landslides. *Reviews of Geophysics*, 34, 33-59.
- HARBITZ, C. B. 1992. Model simulation of tsunamis generated by the Storegga Slides. *Marine Geology*, 105, 1–21.
- HEEZEN, B. C. & EWING, M. 1952. Turbidity currents and submarine slumps, and the 1929 Grand Banks Earthquake. *Am. J. Sci.*, 250, 849–873.
- HILL, J., COLLINS, G. S., AVDIS, A., KRAMER, S. C. & PIGGOTT, M. D. 2014. How does multiscale modelling and inclusion of realistic palaeobathymetry affect numerical simulation of the Storegga Slide tsunami? *Ocean Modelling*, 83, 11-25.
- HURUKAWA, N., TSUJI, Y. & WALUYO, B. 2003. The 1998 Papua New Guinea Earthquake and its Fault Plane Estimated from Relocated Aftershocks. *In: BARDET, J.-P., SYNOLAKIS, C. & OKAL, E. A. (eds.) Pure appl. geophys. 160.*
- IMAMURA, F., GICA, E., TAKASHI, T. & SHUTO, N. 1995. Numerical Simulation of the 1992 Flores Tsunami: Interpretation of Tsunami Phenomena in Northeastern Flores Island and Damage at Babi Island. *Pure and Applied Geophysics*, 144, 555-568.

- JAMELOT, A., GAILLER, A., HEINRICH, P., VALLAGE, A. & CHAMPENOIS, J. 2019. Tsunami Simulations of the Sulawesi Mw 7.5 Event: Comparison of Seismic Sources Issued from a Tsunami Warning Context Versus Post-Event Finite Source. *Pure and Applied Geophysics*.
- JIANG, L. & LEBLOND, P. H. 1992. The coupling of a submarine slide and the surface wave which it generates. *Journal of Geophysical Research*, 97, 12 731–12 744.
- JIANG, L. & LEBLOND, P. H. 1994. Three dimensional modelling of tsunami generation due to submarine mudslide. *J. Phys. Ocean*, 24, 559–573.
- JOHNSON, C. & MADER, C. L. 1994. Modeling of the 105 ka Lanai tsunami. *Sci. Tsunami Hazards* 12, 33-38.
- JOHNSON, J. M. & SATAKE, K. 1997. Estimation of seismic moment and slip distribution of the April 1, 1946 Aleutian tsunami earthquake. *J. Geophys. Res.*, 102, 11 765–11 774.
- KANAMORI, H. 1972. Mechanism of tsunami earthquakes. *Physics of The Earth and Planetary Interiors*, 6, 346-359.
- KAWAMURA, K., SASAKI, T., KANAMATSU, T., SAKAGUCHI, A. & OGAWA, Y. 2012. Large submarine landslides in the Japan Trench: A new scenario for additional tsunami generation. *Geophys. Res. Lett.*, 39, L05308.
- KAWATA, Y., BENSON, B. C., BORRERO, J. L., DAVIES, H. L., DE LANGE, W. P., IMAMURA, F., LETZ, H., NOTT, J. & SYNOLAKIS, C. E. 1999. Tsunami in Papua New Guinea was as intense as first thought. *Eos, Trans. Amer. Geophys. Union*, 80, 101, 104–105.

- KULIKOV, E. A., RABINOVICH, A. B., THOMSON, R. E. & BORNHOLD, B. D. 1996. The landslide tsunami of November 3, 1994, Skagway Harbor, Alaska. *Journal of Geophysical Research: Oceans*, 101, 6609-6615.
- LAY, T. 2018. A review of the rupture characteristics of the 2011 Tohoku-oki Mw 9.1 earthquake. *Tectonophysics*, 733, 4-36.
- LEBLOND, P. H. & JONES, A. 1995. Underwater landslides ineffective at tsunami generation. *Sci. Tsunami Hazards*, 13, 25–26.
- LÓPEZ-VENEGAS, A. M., BRINK, U. S. T. & GEIST, E. L. 2008. Submarine landslide as the source for the October 11, 1918 Mona Passage tsunami: Observations and modeling. *Marine Geology*, 254, 35–46.
- LØVHOLT, F., BONDEVIK, S., LABERG, J. S., KIM, J. & BOYLAN, N. 2017. Some giant submarine landslides do not produce large tsunamis. *Geophysical Research Letters*, 44, 8463-8472.
- LØVHOLT, F., PEDERSEN, G., HARBITZ, C. B., GLIMSDAL, S. & KIM, J. 2015. On the characteristics of landslide tsunamis. *Philosophical Transactions of the Royal Society of London A: Mathematical, Physical and Engineering Sciences*, 373.
- LØVHOLT, F., SCHULTEN, I., MOSHER, D., HARBITZ, C. & KRASTEL, S. 2018. Modelling the 1929 Grand Banks slump and landslide tsunami. *Geological Society, London, Special Publications*, 477.
- MACINNES, B. T., GUSMAN, A. R., LEVEQUE, R. J. & TANIOKA, Y. 2013. Comparison of Earthquake Source Models for the 2011 Tohoku Event Using Tsunami Simulations and Near-Field Observations. *Bulletin of the Seismological Society of America*, 103, 1256-1274.

- MCMURTRY, G. M., FRYER, G. J., TAPPIN, D. R., WILKINSON, I. P., WILLIAMS, M., FIETZK, J., GARBE-SCHOENBERG, D. & WATTS, P. 2004a. Megatsunami deposits on Kohala volcano, Hawaii, from flank collapse of Mauna Loa. . *Geology* 32, 741–744.
- MCMURTRY, G. M., WATTS, P., FRYER, G. J., SMITH, J. R. & IMAMURA, F. 2004b. Giant landslides, mega-tsunamis, and paleo-sea level in the Hawaiian Islands. *Marine Geology* 203, 219-233.
- MOORE, A. L. 2000. Landward fining in onshore gravel as evidence for a late Pleistocene tsunami on Molokai, Hawaii. *Geology*, 28, 247-250.
- MOORE, G. W. & MOORE, J. G. 1988. Large-scale bedforms in boulder gravel produced by giant waves in Hawaii. *Sedimentologic Consequences of Convulsive Geologic Events*. Spec. Pap. Geol. Soc. Am. .
- MOSHER, D. C. & PIPER, D. J. W. 2007. Analysis of multibeam seafloor imagery of the Laurentian Fan and the 1929 Grand Banks landslide area. *In: LYKOUSIS, V., SAKELLARIOU, D. & LOCAT, J. (eds.) Submarine Mass Movements and their Consequences*. Springer.
- MUHARI, A., IMAMURA, F., ARIKAWA, T., HAKIM, A. R. & AFRIYANTO, B. 2018. Solving the Puzzle of the September 2018 Palu, Indonesia, Tsunami Mystery: Clues from the Tsunami Waveform and the Initial Field Survey Data. *Journal of Disaster Research*, sc20181108-sc20181108.
- MURTY, T. S. 1977. Seismic sea waves–tsunamis. *Bull. Fish. Res. Board Can.*, 198, 337.
- NAKATA, K., KATSUMATA, A. & MUHARI, A. 2020. Submarine landslide source models consistent with multiple tsunami records of the 2018 Palu tsunami, Sulawesi, Indonesia. *Earth, Planets and Space*, 72, 44.

- NEWMAN, A. V. & OKAL, E. A. 1998. Teleseismic estimates of radiated seismic energy: The E/M0 discriminant for tsunami earthquakes. *J. Geophys. Res.*, 103, 26885–26898.
- OKADA, Y. 1985. Surface deformation due to shear and tensile faults in a half-space. *Bulletin of the Seismological Society of America*, 75, 1135-1154.
- OMORI, F. 1909. Preliminary report on the Messina–Reggio Earthquake of Dec. 28, 1908. *Bulletin of Imperial Earthquake Investigation Committee* 3(2), 37-46.
- PAKOKSUNG, K., SUPPASRI, A., IMAMURA, F., ATHANASIOS, C., OMANG, A. & MUHARI, A. 2019. Simulation of the Submarine Landslide Tsunami on 28 September 2018 in Palu Bay, Sulawesi Island, Indonesia, Using a Two-Layer Model. *Pure and Applied Geophysics*.
- PIPER, D. J. W., A.N. SHOR & J.E. H. CLARKE 1988. The 1929 Grand Banks earthquake, slump and turbidity current. *Geological Society of America Special Paper*, 229, 77–92.
- RUBIN, K. H., FLETCHER, C. H. & SHERMAN, C. 2000. Fossiliferous Lana'i deposits formed by multiple events rather than a single giant tsunami. *Nature*, 408, 675-681.
- RUFF, L. & KAMAMORI, H. 1980. Seismicity and the Subduction Process. *Phys. Earth Planet. Inter.*, 23, 240-252.
- RUFFMAN, A. & HANN, V. 2006. The Newfoundland Tsunami of November 18, 1929: An Examination of the Twenty-eight Deaths of the “South Coast Disaster”. *Newfoundland and Labrador Studies*, 21, 1719-1726.
- RYAN, W. B. F. & HEEZEN, B. C. 1965. . Ionian Sea Submarine Canyons and the 1908 Messina Turbidity Current *Geological Society of America Bulletin*, 76, 915-932.

- SCHAMBACH, L., GRILLI, S. T. & TAPPIN, D. R. in review. Dual earthquake/landslide source modeling of the 2018 Palu tsunami generation and coastal impact. *Frontiers in Earth Science*.
- SCHAMBACH, L., GRILLI, S. T., TAPPIN, D. R., GANGEMI, M. D. & BARBARO, G. 2020. New simulations and understanding of the 1908 Messina tsunami for a dual seismic and deep submarine mass failure source. *Marine Geology*, 421, 106093.
- SCHULTEN, I., MOSHER, D. C., KRASTEL, S., PIPER, D. J. W. & KIENAST, M. 2018. Surficial sediment failures due to the 1929 Grand Banks Earthquake, St Pierre Slope. *Geological Society, London, Special Publications*, 477.
- SMITH, D. E., FOSTER, I. D. L., LONG, D. & SHI, S. 2007. Reconstructing the pattern and depth of flow onshore in a palaeotsunami from associated deposits. *Sedimentary Geology*, 200, 362-371.
- SOCQUET, A., HOLLINGSWORTH, J., PATHIER, E. & BOUCHON, M. 2019. Evidence of supershear during the 2018 magnitude 7.5 Palu earthquake from space geodesy. *Nature Geoscience*, 12, 192-199.
- SOLHEIM, A., BRYN, P., SEJRUP, H. P., MIENERT, J. & BERG, K. 2005. Ormen Lange—an integrated study for the safe development of a deep-water gas field within the Storegga Slide Complex, NE Atlantic continental margin; executive summary. *Marine and Petroleum Geology*, 22, 1-9.
- SONG, X., ZHANG, Y., SHAN, X., LIU, Y., GONG, W. & QU, C. 2019. Geodetic Observations of the 2018 Mw 7.5 Sulawesi Earthquake and Its Implications for the Kinematics of the Palu Fault. *Geophysical Research Letters*, 46, 4212-4220.
- STEARNS, H. T. 1978. Quaternary shorelines in the Hawaiian Islands. *Bernice P. Bishop Museum Bulletin*, 237, 57pp.

- SWEET, S. & SILVER, E. A. 2003. Tectonics and slumping in the source region of the 1998 Papua New Guinea tsunami from seismic reflection images. *In: BARDET, J., -P., SYNOLAKIS, C. & OKAL, E. A. (eds.) Pure Appl. Geophys., 160.*
- TANIOKA, Y. & SATAKE, K. 1996. Tsunami generation by horizontal displacement of ocean bottom. *Geophys. Res. Lett., 23*, 861-864.
- TAPPIN, D. R. 2017. Tsunamis from submarine landslides. *Geology Today, 33*, 190-200.
- TAPPIN, D. R. 2020. Chapter 54 - Chemosynthetic seep communities triggered by seabed slumping off of northern Papua New Guinea. *In: HARRIS, P. T. & BAKER, E. (eds.) Seafloor Geomorphology as Benthic Habitat (Second Edition).* Elsevier.
- TAPPIN, D. R., GRILLI, S. T., HARRIS, J. C., GELLER, R. J., MASTERLARK, T., KIRBY, J. T., SHI, F., MA, G., THINGBAIJAM, K. K. S. & MAI, P. M. 2014. Did a submarine landslide contribute to the 2011 Tohoku tsunami? *Marine Geology, 357*, 344-361.
- TAPPIN, D. R., MATSUMOTO, T., WATTS, P., SATAKE, K., MCMURTRY, G. M., MATSUYAMA, M., LAFOY, Y., TSUJI, Y., KANAMATSU, T., LUS, W., IWABUCHI, Y., YEH, H., MATSUMOTU, Y., NAKAMURA, M., MAHOI, M., HILL, P., CROOK, K., ANTON, L. & WALSH, J. P. 1999. Sediment slump likely caused 1998 Papua New Guinea Tsunami. *EOS, Transactions of the American Geophysical Union, 80*, 329, 334, 340.
- TAPPIN, D. R., WATTS, P. & GRILLI, S. T. 2008. The Papua New Guinea tsunami of 17 July 1998: anatomy of a catastrophic event. *Nat. Hazards Earth Syst. Sci., 8*, 243-266.
- TAPPIN, D. R., WATTS, P., MCMURTRY, G. M., LAFOY, Y. & MATSUMOTO, T. 2001. The Sissano, Papua New Guinea tsunami of July 1998 — offshore evidence on the source mechanism. *Marine Geology, 175*, 1-23.

- TINTI, S. & ARMIGLIATO, A. 2003 The use of scenarios to evaluate the tsunami impact in southern Italy *Marine Geology* 199 221-243.
- ULRICH, T., VATER, S., MADDEN, E. H., BEHRENS, J., VAN DINTHER, Y., VAN ZELST, I., FIELDING, E. J., LIANG, C. & GABRIEL, A.-A. 2019. Coupled, Physics-Based Modeling Reveals Earthquake Displacements are Critical to the 2018 Palu, Sulawesi Tsunami. *Pure and Applied Geophysics*, 176, 4069-4109.
- WALTER, T. R., HAGHSHENAS HAGHIGHI, M., SCHNEIDER, F. M., COPPOLA, D., MOTAGH, M., SAUL, J., BABEYKO, A., DAHM, T., TROLL, V. R., TILMANN, F., HEIMANN, S., VALADE, S., TRIYONO, R., KHOMARUDIN, R., KARTADINATA, N., LAIOLO, M., MASSIMETTI, F. & GAEBLER, P. 2019. Complex hazard cascade culminating in the Anak Krakatau sector collapse. *Nature Communications*, 10, 4339.
- WATTS, P. 1998. Wavemaker Curves for Tsunamis Generated by Underwater Landslides. *Journal of Waterway, Port, Coastal, and Ocean Engineering*, 124, 127-137.
- WATTS, P., GRILLI, S. T., KIRBY, J. T., FRYER, G. J. & TAPPIN, D. R. 2003. Landslide tsunami case studies using a Boussinesq model and a fully nonlinear tsunami generation model. *Nat. Hazards Earth Syst. Sci.*, 3, 391-402.
- YAMAZAKI, Y., CHEUNG, K. F. & LAY, T. 2018. A Self-Consistent Fault Slip Model for the 2011 Tohoku Earthquake and Tsunami. *Journal of Geophysical Research: Solid Earth*, 0.
- YEH, H., IMAMURA, F., SYNOLAKIS, C., TSUJI, Y., LIU, P. & SHI, S. 1993. The Flores Island tsunamis. *Eos, Transactions American Geophysical Union*, 74, 369-373.
- YEH, H., LIU, P. L.-F., BRIGGS, M. & SYNOLAKIS, C. E. 1994. Propagation and amplification of tsunami at coastal boundaries. *Nature*, 372, 353-355.

FIGURES

Figure 1. Global distribution of mapped oceanic margins and identified submarine landslide generated tsunamis or where these contributed to the event (e.g. Messina). Modified from Tappin 2017).

Figure 2. Digital elevation model of sea-floor relief with bathymetric contours offshore of northern Papua New Guinea looking south (vertical exaggeration $\times 4$). The box shows the slump location in Fig. 4. Inset is location and tectonic framework. Red star is the triggering earthquake. Dashed line along the coast the region of tsunami inundation (Modified from Tappin, 2010).

Figure 3. Amphitheatre area off Sissano lagoon with main morphologic features labeled and photographs of significant seabed features. White and yellow lines define the two amphitheatre headscarps. Red lines are ROV traverses; orange lines are Shinkai Manned Submersible dive traverses. Black dashed line defines the most concentrated region of the biological communities. Scales of inset figures: solid white line=1 m. (From (Tappin, 2020).

Figure 4. 3D cutaway section of the Papua New Guinea slump showing seabed bathymetry and sub-seabed seismic viewed from the northeast (vertical exaggeration $\times 3$). (Reproduced from Tappin et al., 2008. (Reproduced under the Creative Commons Attribution Noncommercial Sharealike 2.5 licence.)

Figure 5. Numerical simulation of 1998 PNG, tsunami source from TOPICS 1.2 combined with the fully nonlinear and dispersive model FUNWAVE with onland runup. Circles measured runups, solid line combined landslide/earthquake mechanism, dashed line earthquake mechanism (Reproduced under the Creative Commons Attribution Noncommercial Sharealike 2.5 licence.)

Figure 6. How submarine landslides generate tsunamis. a. Landslide failure, b. Initial slip and surface drag down above the rear of the landslide, c. Positive and negative wave generation, and d. Landslide movement halts, continued wave propagation.

Figure 7. Digital Elevation Model of the Storegga landslide (EMODnet Bathymetry Consortium (2018): EMODnet Digital Bathymetry (DTM)). Inset map. Location and elevation on tsunami runups on adjacent land areas (Bondevik et al., 2003).

Figure 8. Hawaiian giant landslides. Seabed morphology, locations and extents. Inset shows the Alike Landslide from 120,000 BP (location white box).

Figure 9. Submarine landslides (SMFs) in the region off northern Honshu (Sanriku) coast from pre-March 2011 JAMSTEC bathymetry. Black ellipses: landslides. Red square: the proposed location of the landslide which contributed to the March 2011 tsunami. White ellipse is the location of the submarine landslide identified by Kawamura et al., 2012. The blue dots are the locations of the sites drilled during ODP leg 186. Highest elevation observed tsunami runup/inundation (around 39.5° N) along the Sanriku coast is also marked (From Tappin et al., 2014).

Figure. 10. Digital Elevation Model of Ionian Sea between Sicily and Calabria showing the landslide block that contributed to the Messina 1908 tsunami. (MBES bathymetry from Mem. Descr. Carta Geol. It., vol. XLIV, 216 pp., APAT, Rome, R.). Red outline marks location of Billi et al.' (2008) Landslide; black and white outlines mark proposed location of 1908 submarine landslide, before and after failure. From (From Schambach et al., 2020).

Figure 11. Map of Palu Bay area. Stars are the locations of coastal landslides triggered by the earthquake on 28th September 1981. The bathymetry is a merge of data from Marina et al., (2019) and a scan from Liu et al., (2020). The onland data is Sentinel 2 cloudless data. Inset is the location of the map area.

Figure 12. Tsunami surface elevations for Anak Krakatau collapse, envelope of NHWAVE/FUNWAVE- TVD SE up to 7,610 s. From Grilli et al., 2019).

Figure 13. Anak Krakatau, Sunda Strait. Digital Elevation Model of the landslide blocks resulting from the eruption and collapse on 23rd December 2018. Inset – location map.

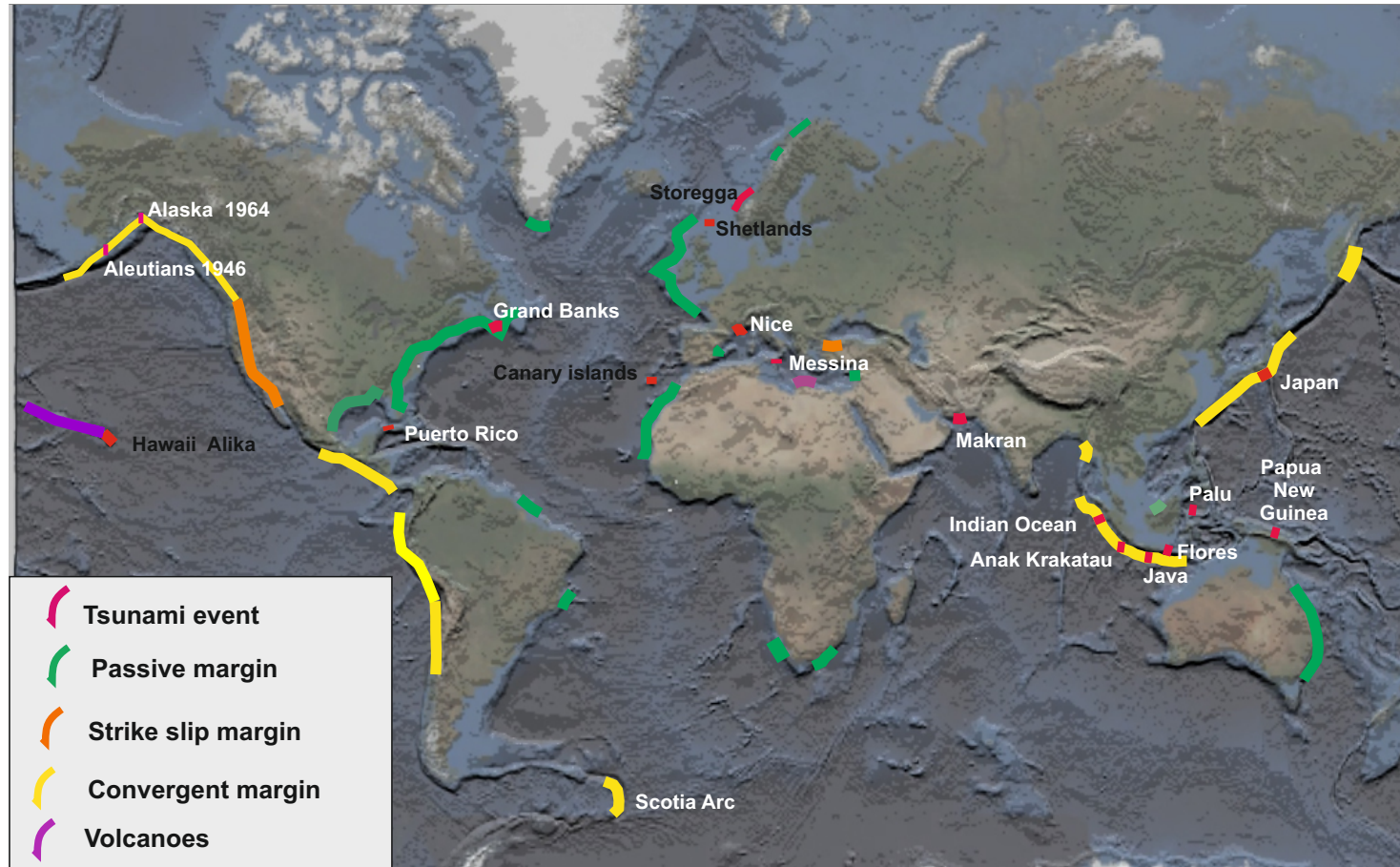


Figure 1. Global distribution of mapped oceanic margins and identified submarine landslide generated tsunamis or where these contributed to the event (e.g. Messina).

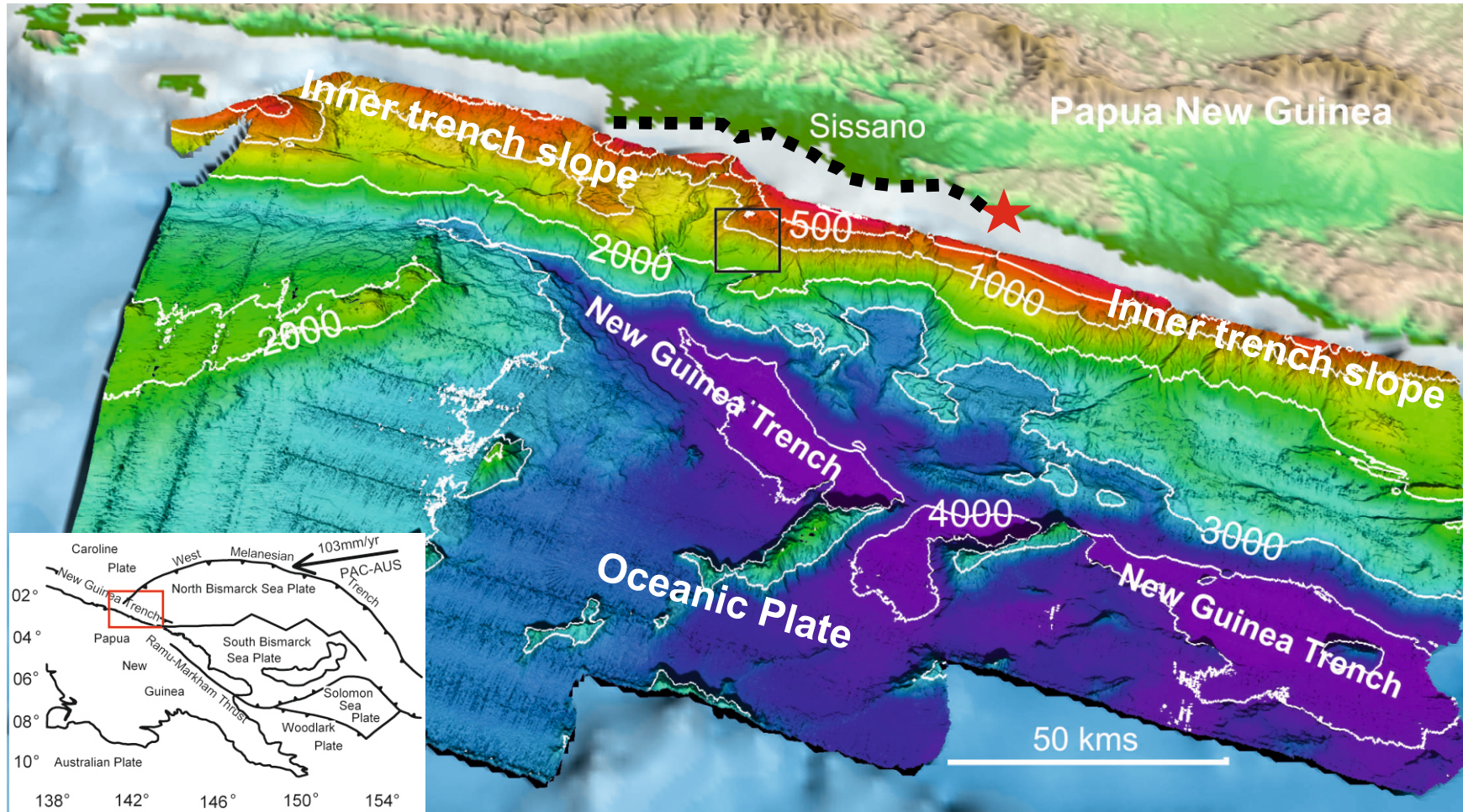


Figure 2. Digital elevation model of sea-floor relief with bathymetric contours offshore of northern Papua New Guinea looking south (vertical exaggeration $\times 4$). The box shows the slump location in Fig. 4. Inset is location and tectonic framework. Red star is the triggering earthquake. Dashed line along the coast the region of tsunami inundation (Modified from Tappin, 2010.)

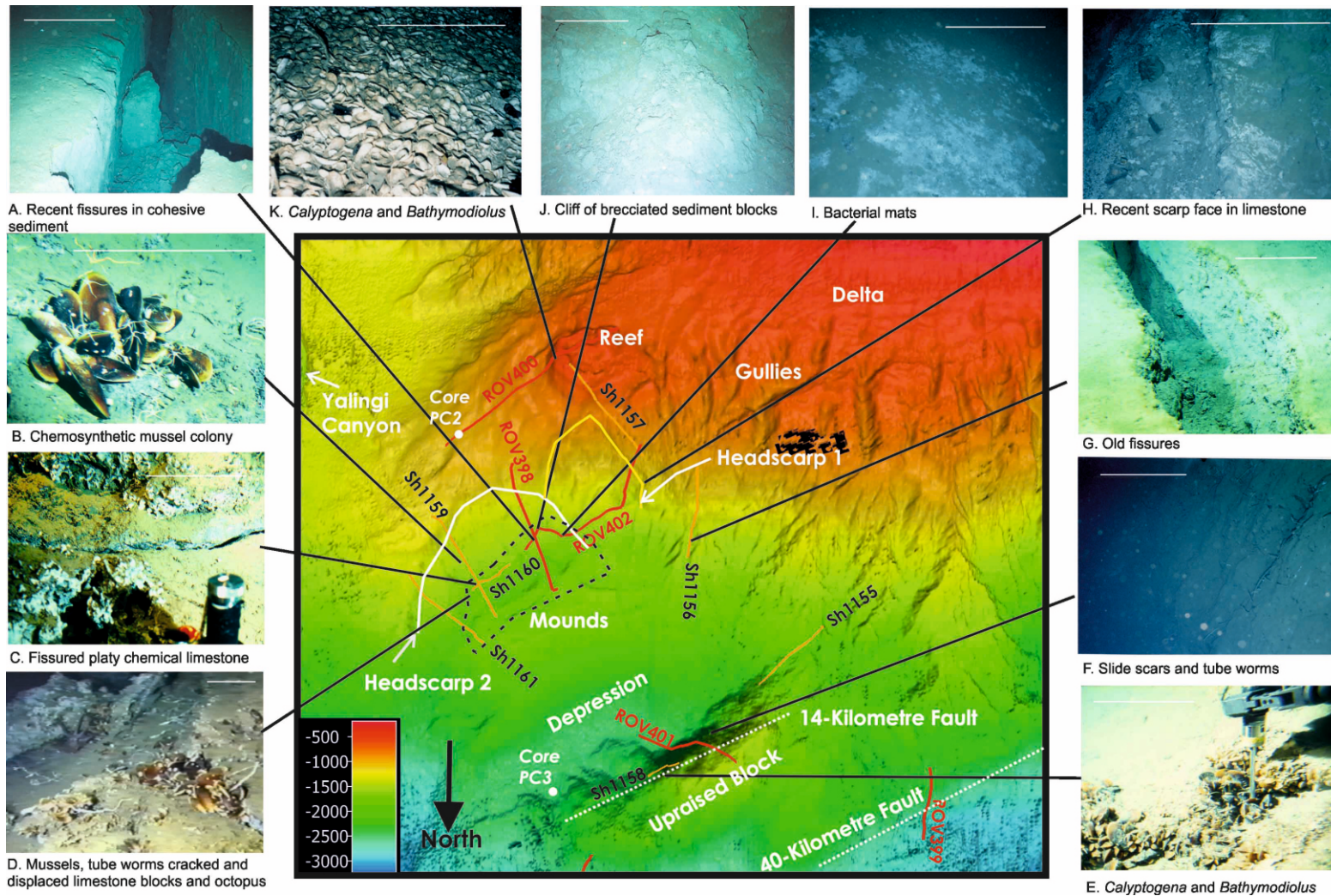


Figure 3. Amphitheatre area off Sissano lagoon with main morphologic features labeled and photographs of significant seabed features. White and yellow lines define the two amphitheatre headscarps. Red lines are ROV traverses; orange lines are Shinkai Manned Submersible dive traverses. Black dashed line defines the most concentrated region of the biological communities. Scales of inset figures: solid white line=1 m.

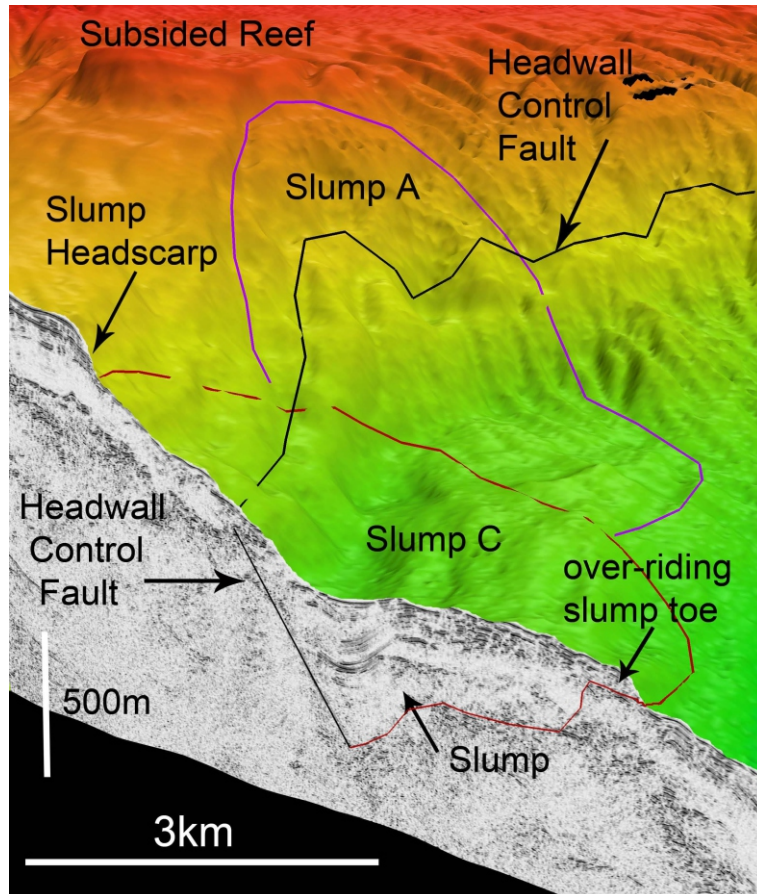


Figure 4. 3D cutaway section of the Papua New Guinea slump showing seabed bathymetry and sub-seabed seismic viewed from the northeast (vertical exaggeration $\times 3$). (Reproduced from Tappin et al., 2008. (Reproduced under the Creative Commons Attribution Noncommercial Sharealike 2.5 licence.)

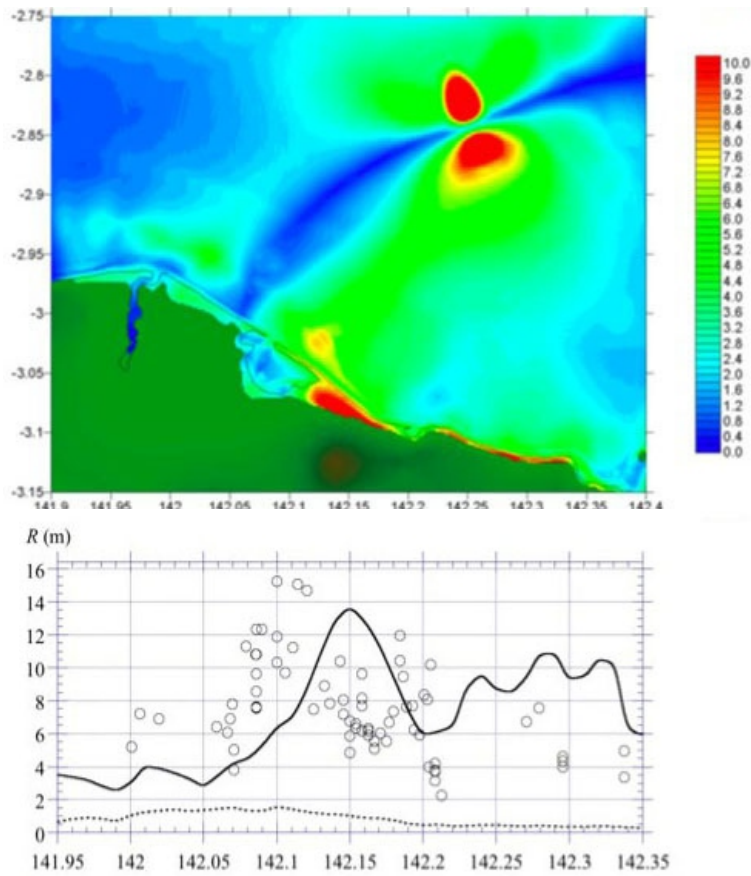


Figure 5. Numerical simulation of 1998 PNG, tsunami source from TOPICS 1.2 combined with the fully nonlinear and dispersive model FUNWAVE with onland runup. Circles measured runups, solid line combined landslide/earthquake mechanism, dashed line earthquake mechanism (Modified from Tappin et al., 2008).

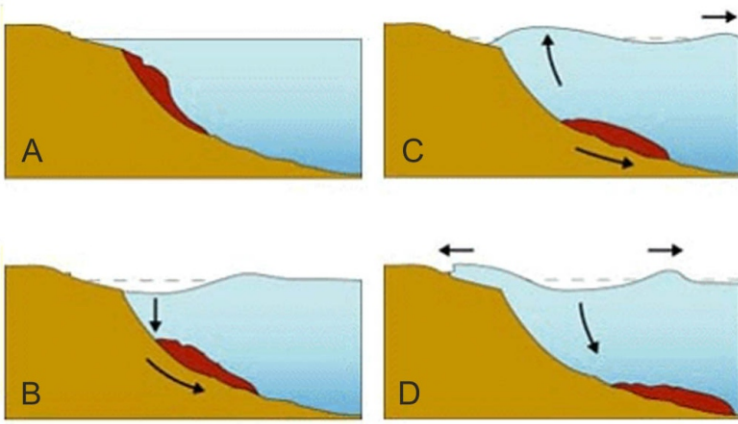


Figure 6. How submarine landslides generate tsunamis. a. Landslide failure, b. Initial slip and surface drag down above the rear of the landslide, c. Positive and negative wave generation, and d. Landslide movement halts, continued wave propagation.

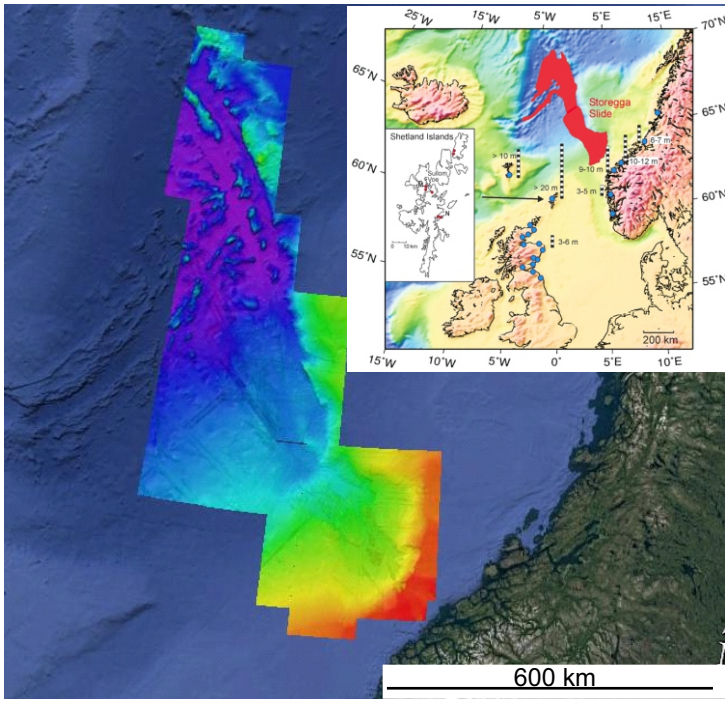


Figure 7. Digital Elevation Model of the Storegga landslide (EMODnet Bathymetry Consortium (2018): EMODnet Digital Bathymetry (DTM)). Inset map. Location and elevation on tsunami runups on adjacent land areas (Bondevik et al., 2003).

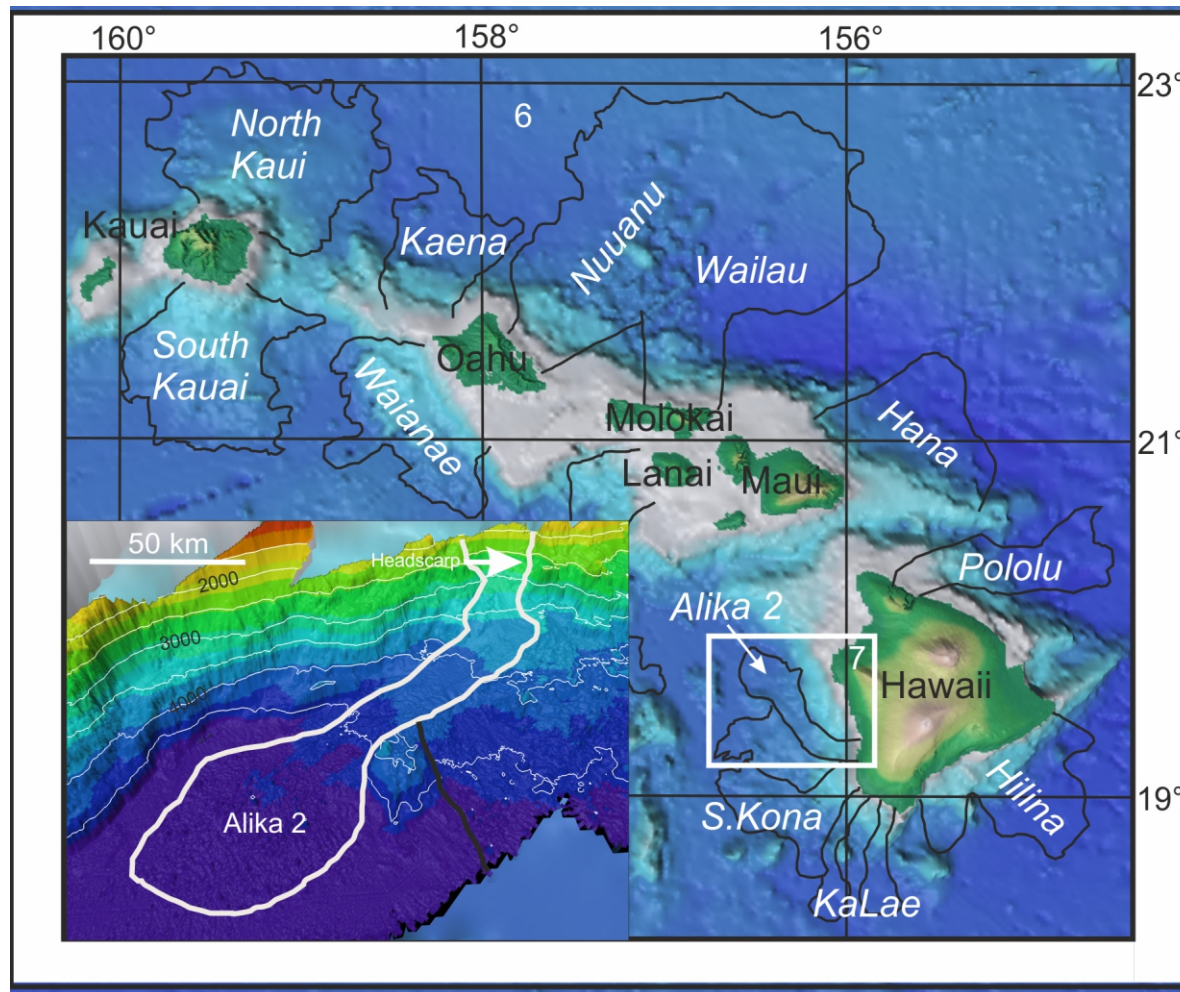


Figure 8. Hawaiian giant landslides. Seabed morphology, locations and extents. Inset shows the Alika Landslide from 120,000 BP (location white box).

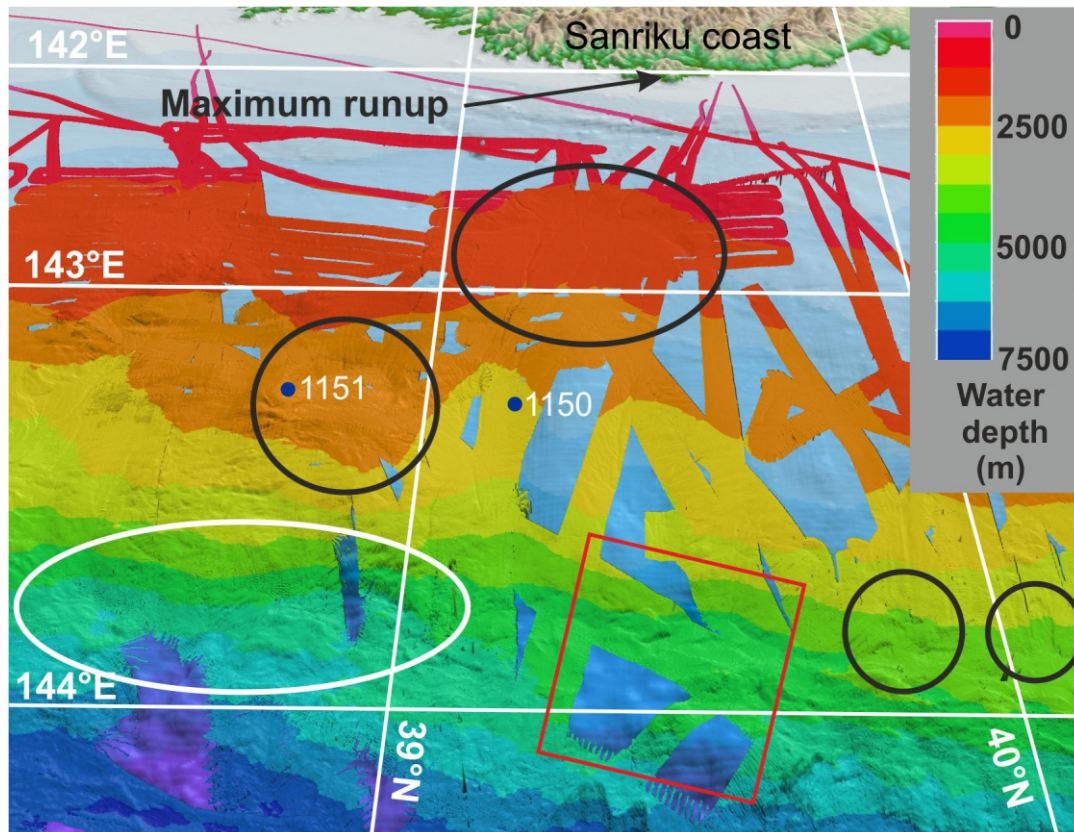


Figure 9. Submarine landslides (SMFs) in the region off northern Honshu (Sanriku) coast from pre-March 2011 JAMSTEC bathymetry. Black ellipses: landslides. Red square: the proposed location of the landslide which contributed to the March 2011 tsunami. White ellipse is the location of the submarine landslide identified by Kawamura et al., 2012. The blue dots are the locations of the sites drilled during ODP leg 186. Highest elevation observed tsunami runup/inundation (around 39.5° N) along the Sanriku coast is also marked..

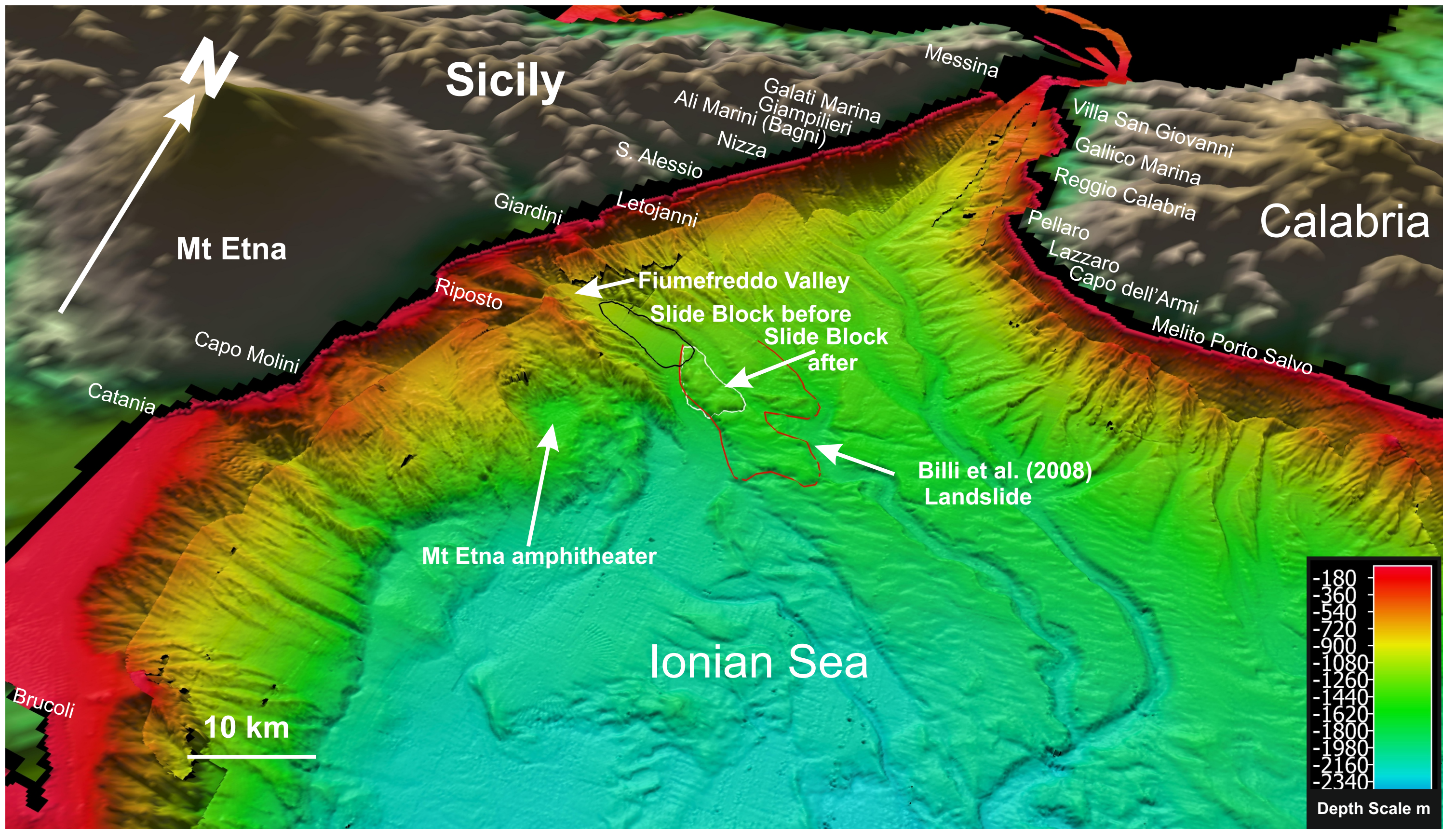


Figure. 10. Digital Elevation Model of Ionian Sea between Sicily and Calabria showing the landslide block that contributed to the Messina 1908 tsunamis. (MBES bathymetry from Mem. Descr. Carta Geol. It., vol. XLIV, 216 pp., APAT, Romeo, R.). Red outline marks location of Billi et al.' (2008) Landslide; black and white outlines mark proposed location of 1908 submarine landslide, before and after failure. From (Schambach et al., 2020).

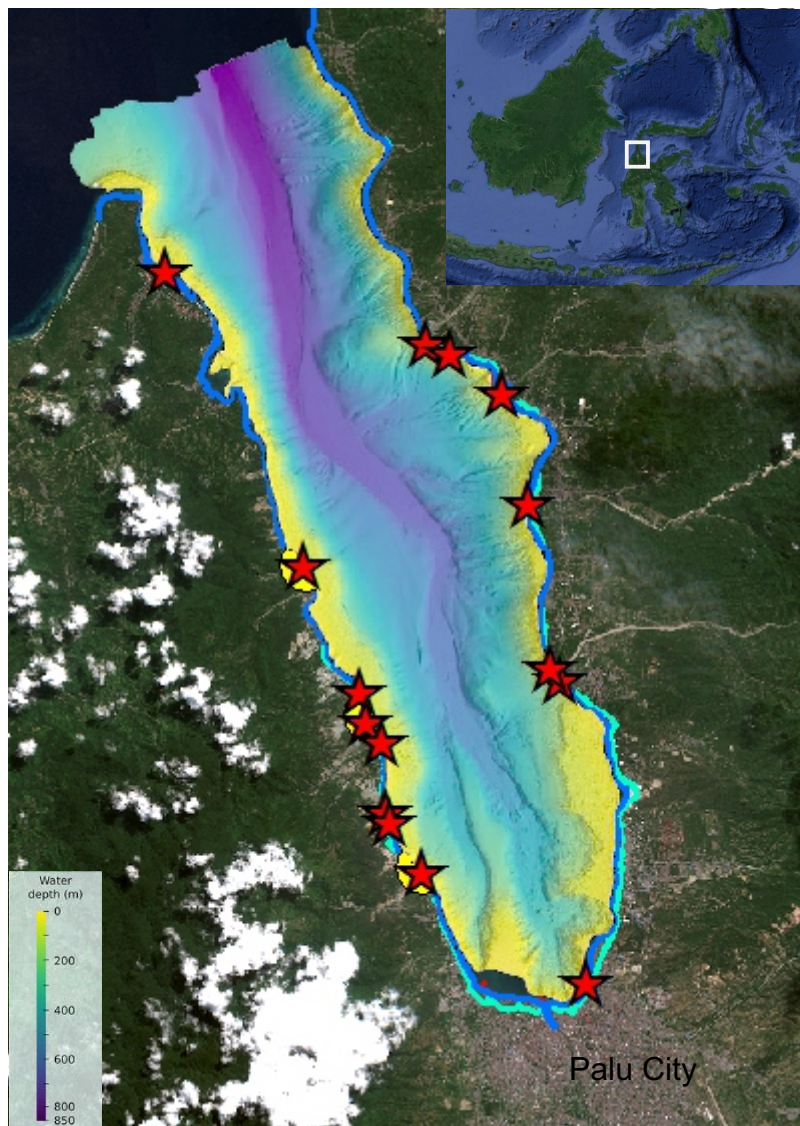


Figure 11. Map of Palu Bay area. Stars are the locations of coastal landslides triggered on 28th September 1981. The bathymetry is a merge of data from Marina et al., 2019 and a scan from Liu et al., 2020. The onland data is Sentinel 2 cloudless data. Inset is the location of the area.

Anak Krakatau η_{\max} at t=7580 s

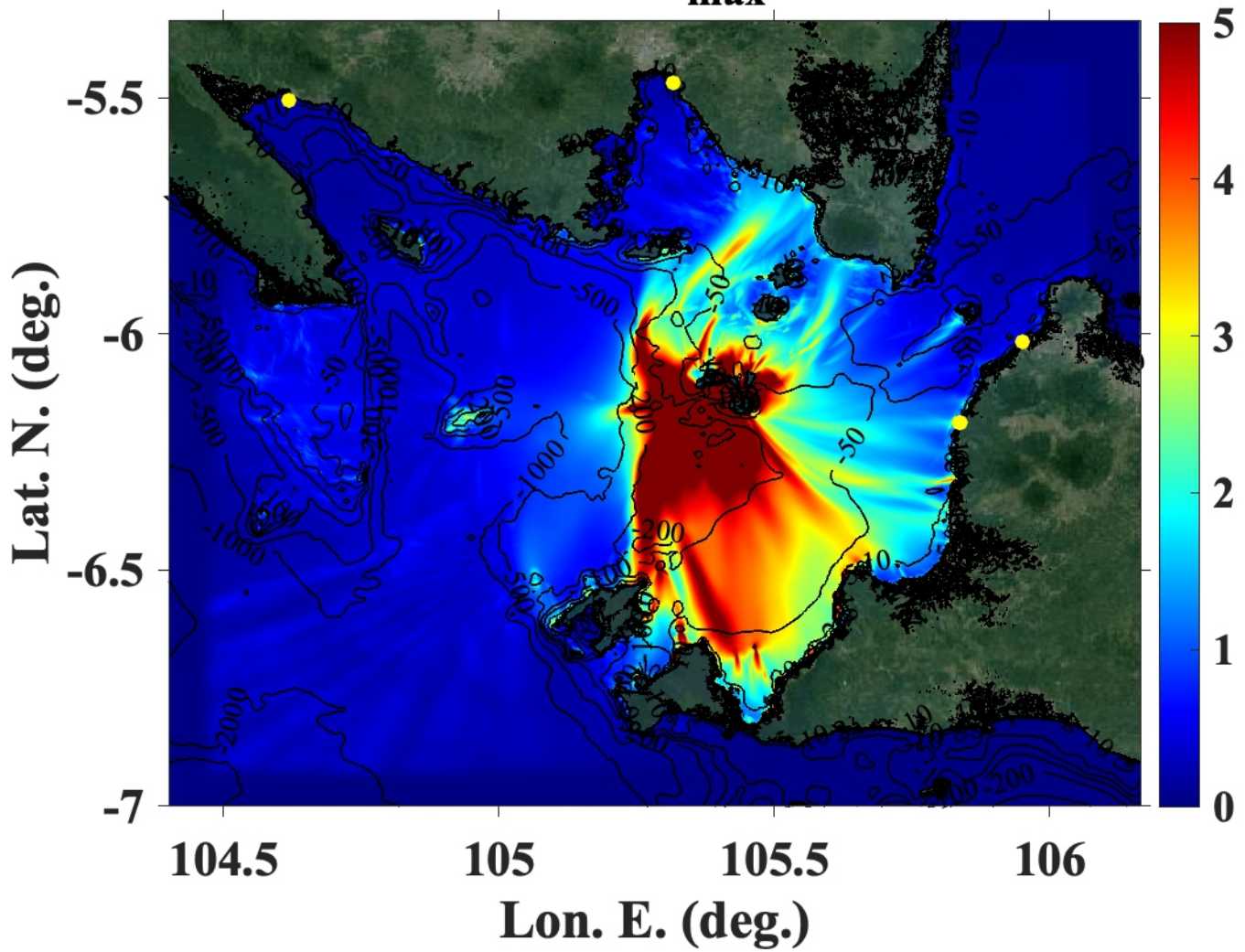


Figure 12. Tsunami surface elevations for Anak Krakatau collapse, envelope of NHWAVE/FUNWAVE- TVD SE up to 7,610 s.

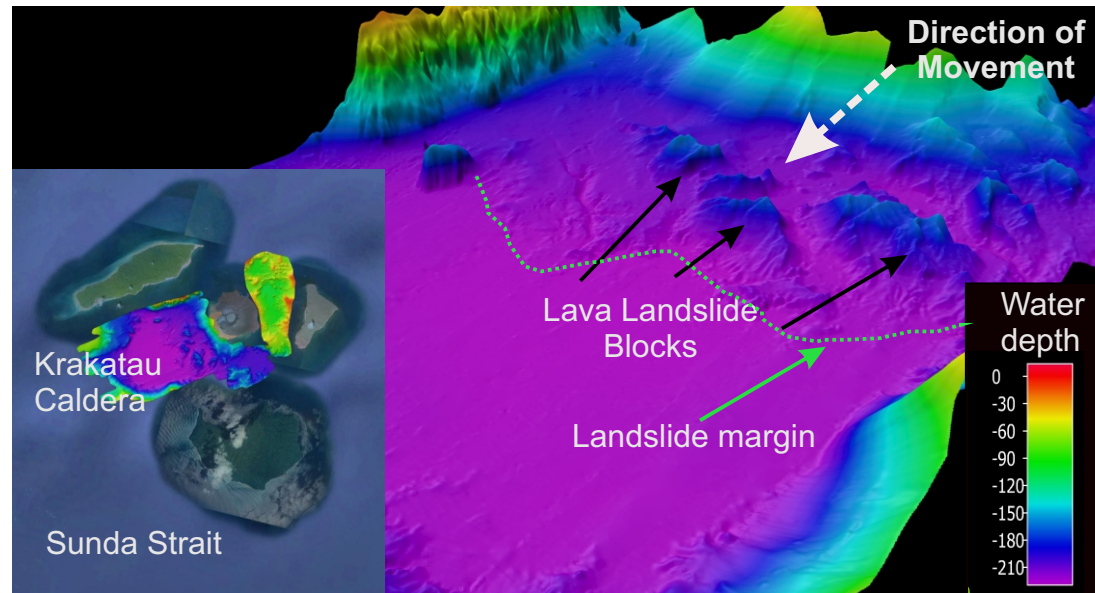


Figure 13. Anak Krakatau, Sunda Strait. Digital Elevation Model of the landslide blocks resulting from the eruption and collapse on 23rd December 2018. Inset – location map.